Phys Chem Minerals (1985) 11:266–283

PHYSICS AND CHEMISTRY OF MINERALS

A Molecular Orbital Study of Bond Length and Angle Variations in Framework Structures

K.L. Geisinger[1]*, G.V. Gibbs[1], and A. Navrotsky[2]

[1] Department of Geological Sciences, Virginia Polytechnic Institute and State University, Blacksburg, Virginia 24061, USA
[2] Department of Chemistry, Arizona State University, Tempe, Arizona 85287, USA

Abstract. Molecular orbital calculations on a variety of silicate and aluminosilicate molecules have been used to explore the bonding forces that govern tetrahedral bond length variations, $r(TO)$, in framework silicates and aluminosilicates. Not only do the calculations provide insight into the variety of structural types and the substitution limits of one tetrahedral atom for another, but they also provide an understanding of the interrelationships among $r(TO)$ and linkage factors, bond strength sum, coordination number, and angles within and between tetrahedra. A study of these interrelationships for a theoretical data set shows that r(SiO) and r(AlO) are linearly correlated with (1) p_o, the bond strength sum to a bridging oxygen, (2) f_s(O), the fractional s-character of a bridging oxygen, and (3) $f_s(T)$, the fractional s-character of the T atom. In a multiple linear regression analysis of the data, 92% of the variation of r(SiO) and 99% of the variation of r(AlO) can be explained in terms of a linear dependence on p_o, f_s(O), and $f_s(T)$. Analogous regression analyses completed for observed r(Al, SiO) bond length data from a number of silica polymorphs and ordered aluminosilicates account for more than 75% of the bond length variation. The lower percentage of bond length variation explained is ascribed in part to the random and systematic errors in the experimental data which have a negligible effect on the theoretical data. The modeling of more than 75% of the variation of r(Al, SiO) in the framework silicates using the same model used for silicate and aluminosilicate molecules strengthens the viewpoint that the bonding forces that govern the shapes of such molecules are quite similar to the forces that govern the shapes of chemically similar groups in solids. The different regression coefficients calculated for $f_s(T)$ indicate that SiO and AlO bond length variations in framework structures should not be treated as a single population in estimating the average Al, Si content of a tetrahedral site.

Introduction

One of the most important and challenging problems in silicate crystal chemistry is the study of the forces that bind atoms into a complex framework of corner-sharing tetrahedra. In important steps toward understanding the effects of these forces, earlier workers established trends among bond lengths, angles, linkage factors, bond strength sums, and coordination numbers which they related in one way or another to a variety of empirical and semi-empirical bonding models (cf., Megaw et al. 1962; Jones and Taylor 1968; Brown et al. 1969; Baur 1970; Phillips et al. 1983; Smith 1974; Ribbe et al. 1974). In an effort to gain an understanding of the nature of these forces, a study of these effects within the context of a non-empirical quantum chemical model would be useful (Carsky and Urban 1980). Currently there are no such computational methods that can be used to study solids as complex as the framework silicates (cf., Chang et al. 1983). On the other hand, if we restrict our studies to local structural phenomena, *molecular orbital* (MO) methods can be used to examine the energetics of these complex structures. The ability of both semi- and non-empirical MO calculations to model local geometries in solid state materials is well-documented (e.g., Gibbs et al. 1972; Tossell and Gibbs 1977, 1978; Newton 1981; Gibbs et al. 1981; Gibbs 1982). Furthermore, the success of these methods strengthens the viewpoint that the bonding forces that govern the shape of a molecule are quite similar to those that govern the shape of a chemically similar group within a solid (Almenningen et al. 1963; Barrow et al. 1979; Gibbs et al. 1981; Gibbs 1982).

The objective of this study is to use the results of non-empirical MO calculations on a variety of representative molecules to explore and systematically analyze trends in bond length and angle variations in studying the bonding forces in framework structures. Since framework structures exist for a variety of crystalline, glassy, and molten silicates and aluminosilicates, these calculations have a wide range of applications (Gibbs 1982; Geisinger 1983; Navrotsky et al., 198). To achieve this objective, energy optimized geometries and energetics of TOT (T=tetrahedral Si, Al, B, Be, Mg) groups in molecules are examined. As a T_2O_7 molecule is the simplest fragment of a framework structure that possesses both four-coodinate T atoms and a bridging oxygen, we have extracted this molecule from the structure as conceptualized in Fig. 1. Protons were attached to its nonbridging oxygens to mimic the local connectedness of a framework and the net effect of the long range field of a periodic array of atoms (Fig. 2a). In the first part of this study, we examine the energetics of the TOT angle in such $H_6T_2O_7$ molecules in terms of the averages and

* *Present address:* Department of Chemistry, Arizona State University, Tempe, Arizona 85287, USA

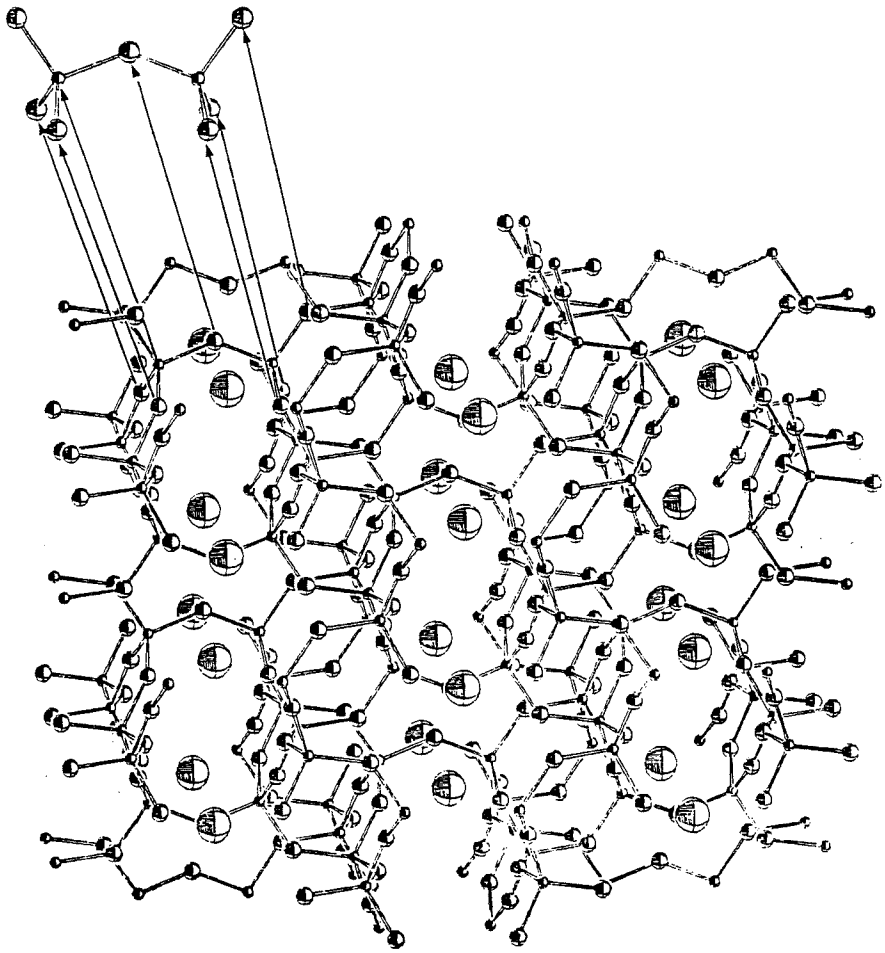

Fig. 1. An ORTEP drawing of a feldspar structure with a representative T_2O_7 unit extracted from the framework. The T_2O_7 unit is representative of the bridging oxygen link common to tetrahedral framework structures. Results of MO calculations on molecules containing the T_2O_7 unit are used to analyze systematically bond length and angle variations in solids

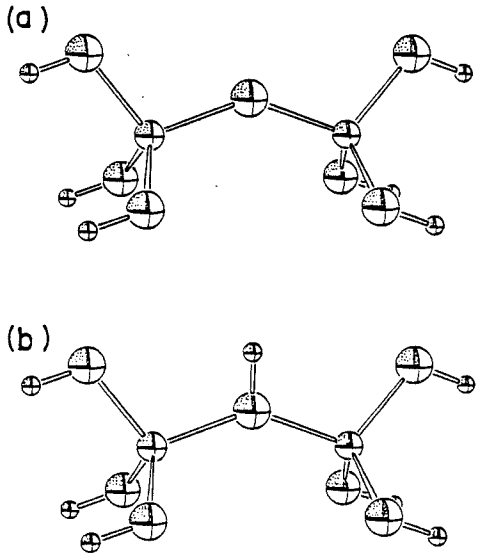

Fig. 2a, b. ORTEP drawings of general conformations of the (a) $H_6T_2O_7$ and (b) $H_7T_2O_7$ molecules. The intermediate-sized spheres represent the tetrahedrally coordinated T atoms (T=Si, Al, Be, B, Mg), the large spheres represent oxygen and the small spheres represent hydrogen. No significance is attached to the relative sizes of the spheres

the ranges of angles observed for framework structures. The results of this analysis provide insight into how chemical composition may place constraints on framework topologies. In addition, the effect on the TOT angle of increased coordination number of the bridging oxygen is examined. Such an increase often occurs when tetrahedral aluminum is charge-compensated by formally monovalent or divalent cations in framework silicates such as feldspar, feldspathoid, cordierite, and stuffed silica derivatives, and in their corresponding glasses.

The second part of the study is devoted to analyzing trends in TO bond length variations as a function of the local environment of the TOT group. Specifically, we assess variations in SiO and AlO bond lengths inasmuch as the majority of the theoretical data has been obtained for molecules containing such bonds. The analysis consists of exploring bond-length perturbing factors (other than Si, Al disorder) that together can provide a good description of SiO and AlO bond length variation in the molecular systems within the confines of linear models. The results of the analysis of the molecular systems are tested against variations of these bond lengths in ordered silicate and aluminosilicate framework structures. The application of these calculations to glassy and molten silicate and aluminosilicate systems will be the subject of a forthcoming paper (Navrotsky et al. 1985).

Computational Details

The majority of the MO calculations reported in this study were undertaken with the Binkley et al. (1980) Gaussian 80 program which performs ab initio MO calculations within the framework of a *linear combination of atomic orbitals* (LCAO). As indicated by Carsky and Urban (1980), ab initio implies that within the LCAO approximation, no further approximations are adopted such as neglect or approximation of integrals with spectroscopic data. It is in this sense that the calculations are considered to be non-empirical. In this study, each calculation was implemented using a minimal STO-3G basis set where each AO is represented by a single *Slater-type orbital* (STO) which in turn is represented by a linear combination of *three Gaussian* (3G) functions (Hehre et al. 1969, 1970). With a STO-3G basis, the Slater exponents zeta (scale factors) for the core functions such as the K-shell for the first-row atoms and the K- and L-shells for the second row atoms are fixed at free atom values. However, the valence-shell zeta values are fixed at *standard molecular* (SM) values as valence-shell exponents for atoms in molecules differ significantly from those for free atoms (Hehre et al. 1969). SM exponents represent an average of energy-optimized exponents determined for a limited set of molecules. During exponent optimization, these molecules were each clamped at a "standard geometry" defined by Pople and Gordon (1967) and extended by Hehre et al. (1970). For example, the SM value for Si was found by averaging optimized values obtained for molecules such as SiH_4, Si_2H_3, and SiH_3CH_3, while the value for O was obtained by averaging values obtained for molecules such as H_2O and CH_2O. SM exponents for first and second row atoms are tabulated by Hehre et al. (1970).

Total molecular energies were calculated using the restricted Hartree-Fock SCF procedure of Roothaan (1951). Based on the principle that the molecular geometry that exhibits the lowest calculated total energy is the equilibrium geometry, bond lengths and angles of each molecule were varied within certain geometry and symmetry constraints until a minimum-energy geometry (referred to as the optimized geometry) was obtained. Nonetheless, because of the nature of the basis functions, the optimized geometries are necessarily basis set dependent. For the minimum STO-3G basis, errors in predicted molecular geometries average about 0.02–0.03 Å for bond lengths and 3–4° for bond angles (Pople 1982; Carsky and Urban 1980). For those molecules optimized using the Gaussian 80 program, a modified conjugate gradient algorithm was employed (Schlegel 1982). On the other hand, for a few $H_7T_2O_7$ molecules that were optimized using the Pople et al. (1973) Gaussian 70 computer program (QCPE 11 236), optimized geometries were determined by completing closely-spaced single-point calculations for various geometries and least-squares-fitting potential energy curves to the single point energies. Comparison of a molecular optimized geometry obtained using the single-point technique to that obtained with gradient optimization shows that careful application of the single-point technique provides results that are essentially identical to those provided by the gradient technique.

Tables 1–4 list the molecules and bond lengths and angles that were optimized in this study. Of the five different types of molecules, the first are the $H_6T_2O_7$ molecules (Table 1) which model bridging two-coordinate oxygen atoms in TOT groups (Fig. 2a). Closely related to these are the $H_7T_2O_7$ molecules (Table 1) shown in Figure 2b which have an additional proton attached to the bridging oxygen. Table 2 contains molecules of the $X(OH)_3$-$H_6T_2O_7$ type shown in Figure 3a which contain the basic *TOT* group but have an additional tetrahedrally-coordinated atom (X = Li, Be, B, C, Na, Mg, Al, Si) attached to the bridging

Table 1. $H_6T_2O_7$ and $H_7T_2O_7$ (T = Si, Al, B, Be, Mg) molecules

Molecules	$r(T_1O)_{br}$	$r(T_1O)_{nbr}$	$r(T_2O)_{br}$	$r(T_2O)_{nbr}$	$\angle T_1OT_2$	$[\angle OT_1O]^a$	$[\angle OT_2O]^a$	E_{total}
$H_6SiBeO_7^{2-}$	1.572 Å	1.685 Å	1.593 Å	1.623 Å	131.0°	109.47°	109.47°	− 820.18203 a.u.
$H_6SiBeO_7^{2-}$	1.568	1.685[b]	1.623	1.623[b]	128.5	116.4	106.2	− 820.19786
$H_6SiBO_7^{1-}$	1.601	1.699	1.436	1.477	125.2	109.47	109.47	− 830.47650
$H_6SiBO_7^{1-}$	1.597	1.699[b]	1.451	1.477[b]	124.2	112.8	107.1	− 830.48084
H_6SiCO_7	1.650	1.657	1.381	1.432	120.8	109.47	109.47	− 843.47042
H_6SiCO_7	1.651	1.657[b]	1.390	1.432[b]	121.4	107.9	107.1	− 843.47321
$H_6SiMgO_7^{2-}$	1.569	1.688	1.859	1.843	137.9	109.47	109.47	−1002.80719
$H_6SiMgO_7^{2-}$	1.566	1.688[b]	1.862	1.843[b]	136.3	114.7	107.5	−1002.78522
$H_6SiAlO_7^{1-}$	1.575	1.671	1.689	1.719	138.6	109.47	109.47	−1045.14313
$H_6SiAlO_7^{1-}$	1.569	1.671[b]	1.695	1.719[b]	138.8	112.8	108.0	−1045.14623
H_6SiSiO_7	1.591	1.658	1.591	1.658	143.7	109.47	109.47	−1091.77364
H_6SiSiO_7	1.594	1.658[b]	1.594	1.658[b]	142.9	108.2	108.2	−1091.77466
$H_6BBO_7^{2-}$	1.405	1.495	1.405	1.495	134.2	109.47	109.47	− 568.99353
$H_6AlAlO_7^{2-}$	1.647	1.739	1.647	1.739	151.3	109.47	109.47	− 998.32842
$H_6AlAlO_7^{2-}$	1.643	1.739[b]	1.643	1.739[b]	151.1	113.2	113.2	− 998.33520
$H_7SiBeO_7^{1-}$[c]	1.65	1.66	1.66	1.58	129.0	109.47	109.47	− 821.038
H_7SiBO_7	1.673	1.651	1.512	1.454	128.0	109.47	109.47	− 831.11549
$H_7SiMgO_7^{1-}$	1.647	1.656	1.951	1.812	136.1	109.47	109.47	−1003.65091
H_7SiAlO_7	1.67	1.65	1.80	1.69	132.0	109.47	109.47	−1045.78316
$H_7SiSiO_7^{1+}$	1.709	1.645	1.709	1.645	132.2	109.47	109.47	−1092.18412
$H_7AlAlO_7^{1-}$	1.76	1.71	1.76	1.71	140.0	109.47	109.47	− 999.22746
$H_7BBO_7^{1-}$	1.49	1.46	1.49	1.46	137.0	109.47	109.47	− 569.87676

[a] Represents average $\angle OTO$. Those $\angle OTO = 109.47°$ were constrained during optimization
[b] Constrained
[c] Downs and Gibbs (1981)

Table 2. $X(OH)_3$–$H_6T_2O_7$ (X = Li, Be, B, C, Na, Mg, Si, Al; T = Si, Al) molecules

Molecules	$r(T_1O)_{br}$	$r(T_1O)_{nbr}$	$r(T_2O)_{br}$	$r(T_2O)_{nbr}$	$(XO)_{br}$	$\angle T_1OT_2$	$[\angle OT_1O]^a$	$[\angle OT_2O]^a$	E_{total}
$Li(OH)_3-SiSiO(OH)_6^{2-}$	1.634 Å	1.660 Å	1.634 Å	1.660 Å	1.945 Å	123.2°	109.47°	109.47°	−1321.82508 a.u.
$Be(OH)_3-SiSiO(OH)_6^{1-}$	1.657	1.656	1.657	1.656	1.703	119.6	109.47	109.47	−1329.42615
$B(OH)_3$–$SiSiO(OH)_6$	1.690	1.650	1.690	1.650	1.528	119.0	109.47	109.47	−1339.50550
$C(OH)_3-SiSiO(OH)_6^{1+}$	1.740	1.646	1.740	1.646	1.438	118.8	109.47	109.47	−1352.26952
$Na(OH)_3-SiSiO(OH)_6^{2-}$	1.621	1.659	1.621	1.659	2.305	128.1	109.47	109.47	−1474.17504
$Mg(OH)_3-SiSiO(OH)_6^{1-}$	1.647	1.654	1.647	1.654	1.995	122.7	109.47	109.47	−1512.03772
$Mg(OH)_3-SiSiO(OH)_6^{1-}$	1.650	1.654	1.650	1.654	1.992	122.4	109.7	109.7	−1512.05833
$Al(OH)_3-SiSiO(OH)_6$	1.676	1.650	1.676	1.650	1.820	119.4	109.47	109.47	−1554.17192
$Al(OH)_3-SiSiO(OH)_6$	1.683	1.650[b]	1.683	1.650[b]	1.827	118.7	107.8	107.8	−1554.18904
$Si(OH)_3-SiSiO(OH)_6^{1+}$	1.714	1.645	1.714	1.645	1.715	117.5	109.47	109.47	−1600.58572
$Li(OH)_3-SiAlO(OH)_6^{3-}$	1.619	1.672	1.750	1.722	1.945[b]	115.7	109.57	109.47	−1274.97285
$Li(OH)_3-SiAlO(OH)_6^{3-}$	1.597	1.676	1.732	1.727	1.945[b]	124.3	112.3	110.8	−1274.99061
$B(OH)_3-SiAlO(OH)_6^{1-}$	1.659	1.657	1.794	1.706	1.492	116.1	109.47	109.47	−1292.93574
$Na(OH)_3-SiAlO(OH)_6^{3-}$	1.617	1.672	1.741	1.720	2.305[b]	116.8	109.47	109.47	−1427.34480
$Mg(OH)_3-SiAlO(OH)_6^{2-}$	1.626	1.664	1.752	1.713	1.964	117.0	109.47	109.47	−1512.03772

[a] Represents average $\angle OTO$. Those $\angle OTO = 109.47°$ were constrained during optimization
[b] Constrained

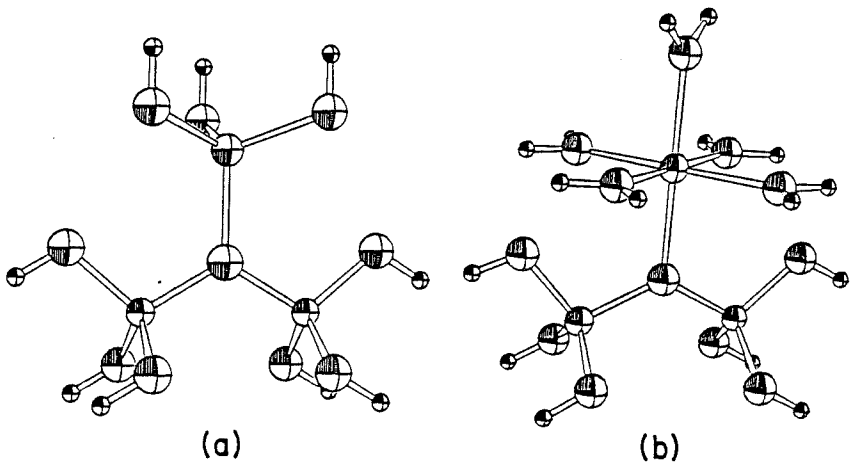

Fig. 3a, b. ORTEP drawings of the general conformations of the (**a**) $X(OH)_3$–$H_6T_2O_7$ and (**b**) $X(H_2O)_5$–$H_6T_2O_7$ molecules. The X atoms modifying the bridging TOT groups are positioned above the bridging oxygens in (**a**) and (**b**). X atoms may include X = Li, Be, B, C, Na, Mg, Al, Si while T atoms are either Si or Al. Intermediate-sized spheres represent the X and T atoms, large spheres represent oxygen, and small spheres represent hydrogen. No significance is attached to the sizes of the spheres

Table 3. $X(H_2O)_5-H_6T_2O_7$ (X = Li, Na, Mg, Al; T = Si, Al) molecules

Molecules	$r(T_1O)_{br}$	$r(T_1O)_{nbr}$	$r(T_2O)_{br}$	$r(T_2O)_{nbr}$	$(XO)_{br}$	$\angle T_1OT_2$	$[\angle OT_1O]^a$	$[\angle OT_2O]^a$	E_{total}
$Li(H_2O)_5-SiSiO(OH)_6^{1+}$	1.645 Å	1.655 Å	1.645 Å	1.655 Å	2.12 Å[b]	123.3°	109.47°	109.47°	−1474.20547 a.u.
$Na(H_2O)_5-SiSiO(OH)_6^{1+}$	1.629	1.655	1.629	1.655	2.38[b]	127.5	109.47	109.47	−1626.62216
$Mg(H_2O)_5-SiSiO(OH)_6^{2+}$	1.661	1.652	1.660	1.652	2.10[b]	122.6	109.47	109.47	−1663.84150
$Li(H_2O)_5-SiAlO(OH)_6$	1.618	1.664	1.729	1.715	2.12[b]	126.3	109.47	109.47	−1427.69836
$Na(H_2O)_5-SiAlO(OH)_6$	1.592	1.664	1.712	1.710	2.35[b]	135.2	110.2	107.0	−1580.01241
$Mg(H_2O)_5-SiAlO(OH)_6^{1+}$	1.632	1.660	1.733	1.710	2.10[b]	128.2	109.47	109.47	−1617.47305
$Mg(H_2O)_5-SiAlO(OH)_6^{1+}$	1.633	1.661	1.758	1.708	2.10[b]	125.4	108.9	104.8	−1617.47964
$Al(H_2O)_5-SiAlO(OH_6^{2+}$	1.671	1.658	1.808	1.706	1.91[b]	124.0	106.7	100.9	−1659.14588

[a] Represents average $\angle OTO$. Those $\angle OTO = 109.47°$ were constrained during optimization
[b] Constrained

oxygen. Table 3 contains data for $X(H_2O)_5$–$H_6T_2O_7$ type molecules (Fig. 3b) which also contain the basic TOT group but have an octahedrally-coordinated atom (X = Li, Na, Mg, Al) attached to the bridging oxygen. For the $H_6T_2O_7$, $X(OH)_3$–$H_6T_2O_7$, and $X(H_2O)_5$–$H_6T_2O_7$ molecules, the attachment of a proton or a four-or six-coordinate X atom to the bridging oxygen models the effects of increased coordination of the bridging oxygen atom. Table 4 lists data for additional molecules which contain an SiOSi group in which the bridging oxygen is only two-coordinate. The conformation of these molecules is very similar to that shown for the $H_6T_2O_7$ molecules in Figure 2a except that the terminal OH groups have been partly or completely replaced by F or Cl atoms, or, in the case of the $(LiO)_2(OH)$ $\cdot SiOSi(OH)(LiO)_2$ and $(NaO)_2(OH)SiOSi(OH)(NaO)_2$ molecules, the lower four hydrogen atoms shown in Figure 2a have been replaced by either Na or Li with optimized SiONa and SiOLi angles of 180°.

Table 4. Other SiOSi molecules containing a two-coordinate bridging oxygen atom

	$r(T_1O)_{br}$	$r(T_2O)_{br}$	∠SiOSi	r(Si...Si)	E_{total}
$F_3SiOSiF_3$	1.577 Å	1.577 Å	158.4°	3.098 Å	−1233.50314 a.u.
$Cl_3SiOSiCl_3$	1.577	1.577	177.7	3.153	−3372.92785
$F_3SiOSi(OH)_3$	1.585	1.587	148.1	3.050	−1162.63919
$Cl_3SiOSi(OH)_3$	1.569	1.597	154.9	3.090	−2232.35668
$(LiO)_2(OH)SiOSi(OH)(LiO)_2$	1.597	1.597	147.0	3.062	−1119.06903
$(NaO)_2(OH)SiOSi(OH)(NaO)_2$	1.614	1.614	156.2	3.159	−1728.71099

As we have chosen to study variation in *TOT* geometry in terms of bridging bond length and angle variations, all TO bridging bond lengths, $r(TO)_{br}$, and bridging *TOT* angles were optimized. For several molecules, nonbridging *TO* bond lengths, *OTO* angles, and *XO* bond lengths were also optimized. Any bond length or angle reported in Tables 1–4 which was fixed during the course of a calculation is indicated. All OH bond lengths were fixed at 0.96 Å and all *OTH* angles were fixed at 109.47°.

TOT Angle Variation

Analyis of TOT Groups with Two-Coordinate Oxygen

Tossell and Gibbs (1978) found that semi-empirical CNDO/2 MO calculations on small molecules of the type H_3SiOTH_3 (T=Si, Al, Be, B) can be used to model Si*OT* angle variations in silicates. As an extension of that study, we have examined bridging *TOT* angles calculated using non-empirical MO techniques for the $H_6T_2O_7$ molecules listed in Table 1. The optimized angles for several molecules with two-coordinate bridging oxygens, compared in Table 5 to average observed bridging angles in solids, do a good job in modeling average bridging angles in solids, providing the molecular model is adequate. However, in the case of the BOB, SiOMg, and AlOAl groups. the simple $H_6T_2O_7$ molecule as a model for solids may not be adequate as will be discussed later.

Energy variation as a function of the *TOT* angles for some of these $H_6T_2O_7$ molecules has been generated by fixing all bond lengths and remaining angles at their optimized or constrained values and then performing single point calculations at various *TOT* angles. Comparison of the shapes of the potential energy curves (upper solid-line curves, Fig. 4) to frequency distributions of observed angles in solids (histogram inserts, Fig. 4) suggests that the shapes of these curves for two-coordinate bridging oxygen atoms in molecules may provide an indication of the range of observable angles in solids. For example, the SiOSi and SiOAl groups have relatively flat potential curves and correspondingly wide distributions of observed angles. In contrast, the SiOB and SiOBe potential curves have deeper potential wells in agreement with the smaller ranges of angles as observed in solids (Tossell and Gibbs 1978).

We summarize these particular observations by plotting the range of observed Si*OT* (T=Be, B, Al, Si) angles in solids as a function of barrier to linearity calculated from the molecular potential energy curves (Fig. 5). The barrier to linearity is defined to be the difference between the total energy of the molecule calculated at a bridging *TOT* angle of 180° and that calculated at the optimized *TOT* angle. Thus, it is a measure of the depth of the potential well for each curve (Fig. 4). Not only does the depth of the well shed light on the energetics of the angle, but it also sheds light on the flexibility of the angle, the shallower the well, the more flexible the angle. In Figure 5, we see that the greater the barrier to linearity (and therefore the less flexible the Si*OT* angle), the smaller the range of observed angles in solids. For the four data points in Figure 5, a linear correlation of angular range with barrier to linearity fits the data well.

Table 5. Comparison of calculated minimum energy *TOT* angles in $H_6T_2O_7$ groups and average *TOT* angles in solids

TOT group	Minimum energy angle in $H_6T_2O_7$ molecules	Average angle in solids
SiOSi	144°	145°
SiOAl	139	138
SiOB	125	129
SiOBe	131	127
SiOMg	138	118
BOB	134	119
AlOAl	151	133

It may be argued that this correlation is perhaps fortuitous because it does not hold for all the curves presented in Figure 4. However, as observed by Gupta and Tossell (1983), one cannot expect close correspondence between non-empirical calculated "observations" and experimental data if the experimental data are perturbed by factors external to the molecular group used as a model. Particularly in the case of the BOB, SiOMg, and AlOAl groups, the $H_6T_2O_7$ molecule may be an inadequate model for the local environment in solids because it does not take into account additional perturbing factors which commonly occur in the solids. For example, the two-coordinate oxygen in each of these *TOT* groups is underbonded in the sense that the Pauling bond strength sum to the atom (p_o) is only 1.5. Also, the bridging oxygen of these groups in solids is usually coordinated to one or more non-tetrahedral atoms. As will be shown in the next section, additional atoms coordinated to the bridging oxygen perturb the *TOT* angle, which might be relatively flexible when the oxygen is two-coordinate, toward a narrower average angle and a more restricted range of angles. Admittedly, the bridging oxygen of the SiOBe group is equally underbonded in H_6SiBeO_7 and usually coordinated to an additional atom or atoms in beryllosilicates, but we still see fair agreement between our non-empirical results and the experimental data. However, the two-coordinate SiOBe group contains a narrow minimum-energy angle which is fairly inflexible to begin with. Thus, it may not be overly affected by these "external" atoms (Downs and Gibbs 1981).

Factors other than the effect of a three-coordinate oxygen must also be considered in the BOB and SiOMg groups

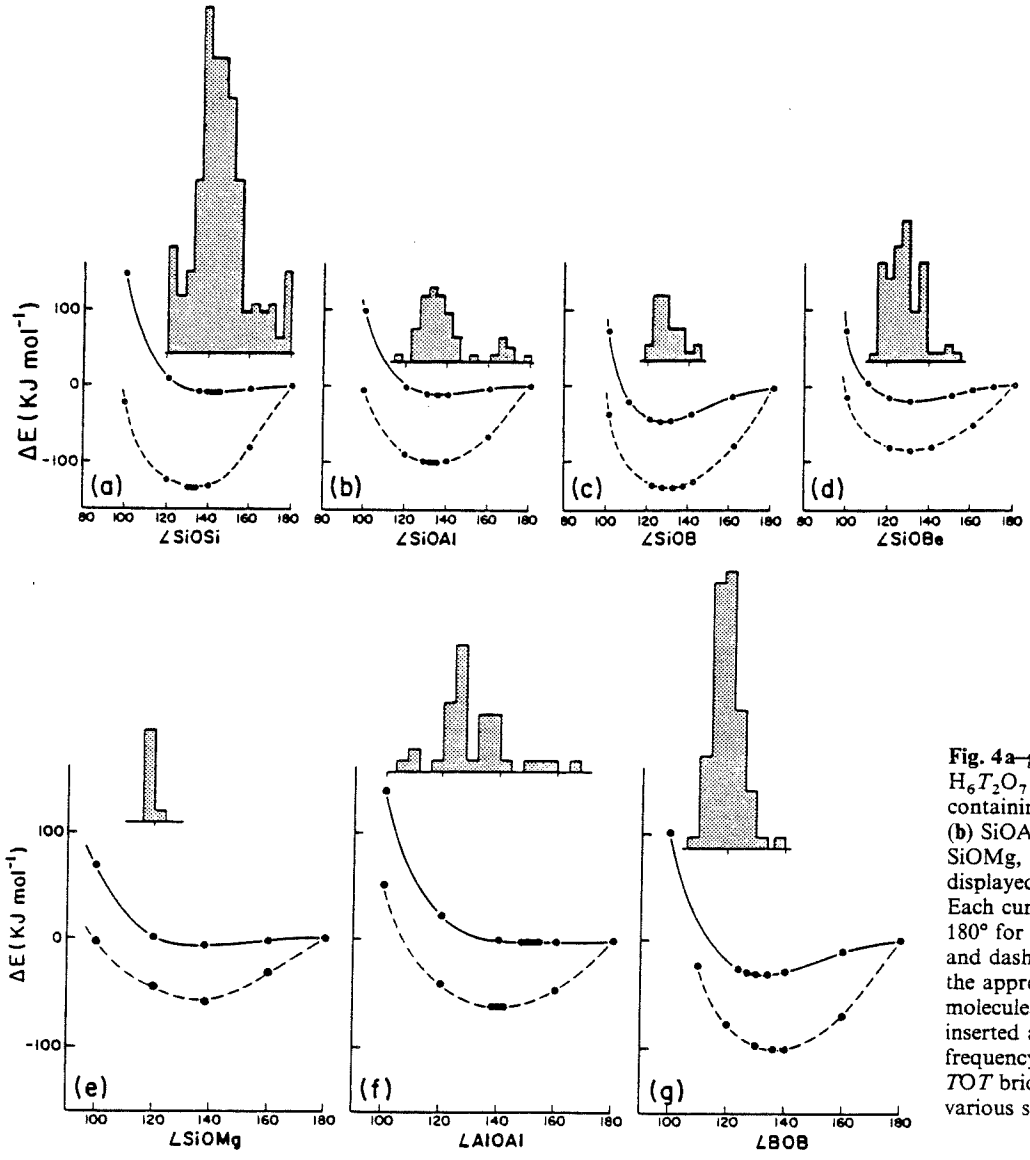

Fig. 4a–g. Potential energy curves for $H_6T_2O_7$ and $H_7T_2O_7$ molecules containing the TOT groups (**a**) SiOSi, (**b**) SiOAl, (**c**) SiOB, (**d**) SiOBe, (**e**) SiOMg, (**f**) AlOAl, and (**g**) BOB displayed as a function of TOT angles. Each curve is referenced to $\Delta E = 0$ at 180° for ease of comparison. The solid and dashed curves were calculated for the appropriate $H_6T_2O_7$ and $H_7T_2O_7$ molecules, respectively. The histograms inserted above each pair of curves is a frequency distribution of experimental TOT bridging angles observed in various solids

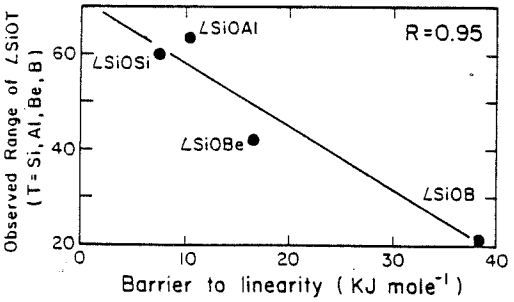

Fig. 5. Observed ranges of experimental SiOT bridging angles (T= Si, Al, Be, B) in various silicates plotted as a function of barrier to linearity. Barrier to linearity is the difference in total energy between the H_6SiTO_7 molecule at its optimized geometry and at a geometry with an SiOT bridging angles of 180°

when comparing calculated to observed data. Not only is the bridging oxygen in $H_6B_2O_7$ underbonded, but corner-sharing borate tetrahedra are often linked together into a three-membered ring consisting of the two such tetrahedra and a borate triangle. These three-membered rings require narrow BOB angles resulting in strain and poor agreement between information provided from calculations on $H_6B_2O_7$ and what we observe in solids. Magnesiosilicates present a more difficult problem because such solids with four-coordinate Mg and Si are comparatively rare. The lack of correspondence between calculated and observed data may very well be partly due to a very restricted experimental data set.

Considering the correspondence between barriers to linearity for two-coordinate oxygen molecules and observed ranges of certain TOT angles in solids (and the fact that we can rationalize the lack of correspondence for other TOT groups), the type of tetrahedral atom may place some constraint on the structure type and substitutional limits of one tetrahedral atom for another simply in terms of the range of energetically feasible TOT angles. In support of this, we examine the observed distributions of some tetrahedral atoms in a few framework silicates. It is well known that Al and Si substitute rather freely for one another in framework aluminosilicates (as long as proper charge-balance occurs) and that there is a wide variety of aluminosili-

cate structure types such as feldspar, paracelsian, feldspathoid, cordierite and zeolite. These observations are in agreement with the very similar and flat potential energy curves for the SiOSi, SiOAl, and AlOAl groups in the $H_6T_2O_7$ molecules (Gibbs et al. 1981). On the other hand, there are relatively few documented borosilicate framework structure types (with B in tetrahedral coordination). These include reedmergnerite ($NaBSi_3O_8$) (Eugster and McIver 1959; Appleman and Clark 1965), the boron analogue of low albite; $KBSi_3O_8$, the boron analogue of low microcline, and danburite ($CaB_2Si_2O_8$) (Phillips et al. 1974) which is structurally similar to anorthite. Low albite exhibits a relatively wide range of TOT angles from ~130 to 161° (31°) with the SiOAl angles ranging only from ~130 to 142° (12°). Low microcline exhibits a range of TOT angles from ~131 to 155° (24°) with the SiOAl angles ranging from ~131 to 151° (20°). The TOT angles in reedmergnerite range from ~125 to 158° (23°) with the SiOB angles ranging from ~125 to 143° (18°). No TOT data are available for $KBSi_3O_8$. In view of the rather more restricted range of SiOAl angles in the alkali-feldspar structures when compared to a possible range on the order of 65° (from Fig. 5), it is not surprising to see boron analogues of these structures. They fit the requirements of the SiOB group having a restricted angular range on the order of 22° (from Fig. 5). In contrast, anorthite, which contains only SiOAl groups, exhibits a wide range of angles from ~123° to ~170° (47°). At first glance, the existence of a framework structure such as danburite with composition $CaB_2Si_2O_8$ seems contrary to our interpretation of the theoretical potential energy curves. However, danburite is structurally similar, but not isostructural with anorthite. The range of SiOB angles in danburite is from ~126 to 137° (11°), a small range with a fairly narrow average angle (129°) in agreement with the potential curve for H_6SiBO_7. Furthermore, whereas anorthite consists entirely of SiOAl groups, danburite contains an SiOSi and a BOB group as well as SiOB group. Interestingly, the more flexible SiOSi group has the widest TOT angle (137°) in the structure. We can infer that the B and Si atoms in danburite are distributed in a fashion that conforms with the restrictions implied by the potential energy curves for the $H_6T_2O_7$ molecules. A borosilicate framework topologically equivalent to anorthite is possibly unstable relative to that of danburite because of the wide range of SiOB angles required for the anorthite structure.

Another framework silicate whose structure is of interest is low cordierite ($Mg_2Al_4Si_5O_{18}$). The six membered ring in this mineral has an average TOT angle of 173° (Gibbs 1966; Cohen et al. 1977) whereas the remaining TOT angles of the four-membered rings average 129°. The Al and Si are ordered into both the four- and six-membered rings in agreement with the flat potential curves for $H_6Si_2O_7$ and H_6SiAlO_7. One would predict the substitution of B for Al in this structure to be limited to the four-membered ring, giving a maximum substitution of two boron atoms per formula unit. It is unlikely, in view of the wide angles required, that B could substitute for Al in the six-membered ring. In comparison, we can examine the distribution of Be and Si in beryl ($Al_2Be_3Si_6O_{18}$), which is isostructural with indialite, a highly disordered polymorph of $Mg_2Al_4Si_5O_{18}$ (Meagher and Gibbs 1977). The potential curve for H_6SiBeO_7 suggests that like B, Be atoms should be restricted in general to narrow TOT angles as observed in beryl. Only Si participates in the six-membered ring with an average SiOSi angle of 168° (Gibbs et al. 1968), whereas Be is ordered into the four-membered rings that link the six-membered rings into a framework with an average SiOBe angle of 127°.

Based on Cruickshank's (1961) d–p π-bonding model, Brown and Gibbs (1970) made the proposal that Si should prefer those tetrahedral sites in a framework silicate that are involved in the wider TOT angles and that Al, B, Be, and Mg should prefer those involved in narrower average TOT angles. It was argued that bonds of larger π-bond order (i.e., SiO) should be shorter and comprise wider TOT angles. Although Si tends to be ordered into these tetrahedra in the framework silicates, Brown and Gibbs (1970) also found in the non-framework silicates contrary to their proposal that Si was more than often ordered into the tetrahedra with smaller average TOT angles. This ordering scheme is sensible if we view the ordering of tetrahedral atoms in terms of our potential energy curves for two-coordinate TOT groups. Since the potential curve for the SiOSi curve is very flat, wider SiOSi angles are not much different energetically than narrow SiOSi angles. If we attempt to rationalize the broad range of silicate structures containing SiOSi groups in terms of the d–p π-bonding model, we would fail for the same reason that the Brown-Gibbs proposal fails for non-framework silicates. It does not provide for narrow SiOSi angles. In contrast, the flat potential curve for SiOSi helps to rationalize the broad range of SiOSi angles required to conform with a wide range of structure types exhibited by silicates (Newton and Gibbs 1980; Gibbs et al. 1981). Nonetheless, the potential energy curves for the SiOT angles (T=Al, B, Mg, Be) displayed in Figure 4 show minima 5 to 20° narrower than that calculated for the SiOSi angle in conformity with the proposal that Si should prefer those tetrahedral sites involved in wider angles.

Effects of Increasing the Coordination of the Bridging Oxygen

The addition of a proton to the bridging oxygen in the $H_7T_2O_7$ molecules (Table 1, Fig. 2b) roughly models the effect of increasing the coordination of the bridging oxygen. Comparison of the minimum energy TOT angles for the $H_7T_2O_7$ groups to those in related $H_6T_2O_7$ groups (Table 1) does not show any consistent change for the TOT groups examined. The flexible SiOSi, SiOAl and AlOAl groups in the $H_6T_2O_7$ molecules show a marked decrease in the TOT angle with an increase in coordination. In contrast, the bridging angles for SiOB, SiOBe, BOB and SiOMg show little change with increased coordination. Tossell (1984) suggests that the optimized TOT angle in the protonated ($H_7T_2O_7$) molecules is determined by the more rigid requirement of the TOH angle to have a fairly narrow angle (110–115°).

Examination of the potential energy curves as a function of the TOT angle generated for several of the $H_7T_2O_7$ molecules (lower dashed-line curves, Fig. 4) does show a consistent trend for all the TOT groups. In every case, the potential well for the $H_7T_2O_7$ molecule is deeper than for the corresponding $H_6T_2O_7$ molecule. Thus, the barrier to linearity is greater for the three-coordinate oxygen angles than for the two-coordinate angles, suggesting that increased coordination of the bridging oxygen in a given TOT group will restrict the range of energetically feasible angles.

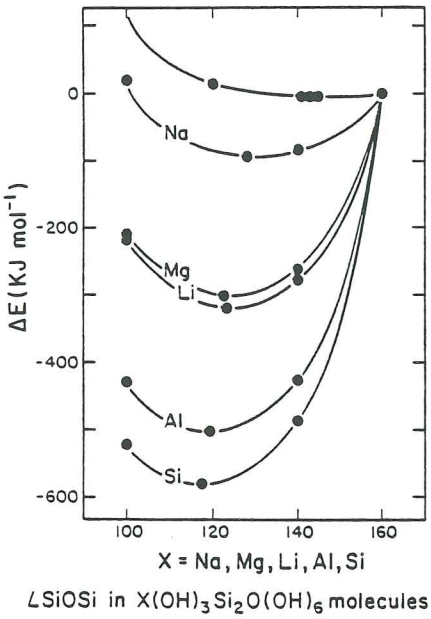

Fig. 6. Potential energy curves for $X(OH)_3$–$H_6Si_2O_7$ molecules (X=Na, Mg, Li, Al, Si) displayed as a function of SiOSi angle. Each curve is referenced to $\Delta E=0$ at 160° for ease of comparison. The potential energy curve for $H_6Si_2O_7$ (top curve) is displayed for comparison of the two-coordinate oxygen curve to three-coordinate oxygen curves

Ranges in SiOSi and SiOAl angles in framework silicates are in agreement with this interpretation. Two-coordinate SiOSi angles range from 131 to 180° whereas three-coordinate SiOSi angles only range between 129 and 152°. In SiOAl groups, two-coordinate angles range from 131 to 176°; three-coordinate angles range from 123 to 151°. Similar ranges have been observed for the disilicates (Gibbs 1982). The potential energy curves in Figure 4 also suggest that the bending force constant of a TOT group with a three-coordinate oxygen atom will be significantly larger than that for a group with a two-coordinate oxygen.

The degree to which the angular range of a given TOT group is restricted by increased coordination may depend on the (chemical) type of the additional coordinating atom. This is suggested by potential energy curves (Fig. 6) for some of the $X(OH)_3$–$H_6Si_2O_7$ molecules listed in Table 2. The barrier to linearity for the SiOSi angle in these molecules increases substantially in the sequence X=Na, Mg, Al, Si; i.e. moving from left to right within one row of the periodic table. Comparison of the potential curves for X=Na and X=Li also suggest that for atoms within one column, coordinating an atom higher in the column to the bridging oxygen will result in a larger barrier to linearity. Whether these trends can be observed in solids is questionable. When one compares X-AlOSi (X=Na, Mg, K, Ca, Sr, Ba) groups in a variety of framework aluminosilicates, the ranges in AlOSi angles do not exhibit any trend related to the type of nonframework X atom. On the other hand, one can restrict the comparison to AlOSi angles in topologically identical structures where one expects similar angles. For example, the range of Na–AlOSi angles in low albite is only ~12° whereas the range of corresponding K–AlOSi angles in low microcline is ~20°. This is in agreement with the interpretation of the potential energy curves that Na should have a more restrictive effect on the TOT angle than K. At this point, we recognize that the requirements of strict periodicity in different crystalline materials must impose additional constraints on local geometry that may compete with the "optimization" of that local geometry within the solid.

TO(T=Si, Al) Bond Length Variation

Factors Related to SiO and AlO Bond Length Variation

The objective of this part of the study is to analyze those factors in the local environment around a tetrahedral SiO or AlO bond that can be related to bond length variation. When itemizing such factors, the average Al-content of a tetrahedron of a structure has the most pronounced effect on the mean TO bond length $<r(TO)>$ (Cole et al. 1949; Smith 1954; Smith and Bailey 1963). The linear relationship between average Al-content and $<r(TO)>$ established by Smith (1954) and later revised by Smith and Bailey (1963), Jones (1968), and Ribbe and Gibbs (1969) has proven useful in estimating average Si/Al site populations. However, these authors and others stress that such a model cannot be strictly accurate in estimating average Al contents of individual tetrahedra because the effects of local environment (other than chemical content of the tetrahedron) are not explicity included. In this study, we are primarily concerned with evaluating these other local environmental effects on SiO and AlO bond lengths as an understanding of these is prerequisite to understanding the effects of Al/Si disorder.

Previous investigations have related $r(TO)$ variation in silicates to a variety of factors (parameterized in different fashions), many of which are described by Brown et al. (1969) and Ribbe et al. (1974). Broadly summarizing these bond-length perturbing factors, we have (1) coordination number of the bridging oxygen; (2) type of adjacent tetrahedral atom, i.e. the "linkage factor"; (3) type of nontetrahedral atoms and their distances away from the bridging oxygen; (4) variation of bridging TOT angles; and (5) variation of tetrahedral OTO angles. These factors may be subdivided into only two groups. The first reflects the local coordinating environment around the TO bond in terms of nontetrahedral and/or tetrahedral atoms. The second group reflects the angular environment.

Having summarized the general types of observable factors, the problem is to determine how to simply parameterize these factors to provide a good model of AlO and SiO bond length variation in framework structures as a general group. In a previous study of this type, Swanson et al. (1980) and Swanson (1980) successfully devised an empirical model of r(Si, AlO) variation in framework silicates using: (1) the sum of the Pauling bond strengths to the bridging oxygen p_o; (2) the fractional s-character of the bridging oxygen $f_s(O)=1/(1\text{-sec}\angle TOT)$, and (3) the average Al-content of the tetrahedon x, because they chose to treat the different bond types as a single population. Referring back to the different types of parameters which influence bond length variation, we see that Swanson et al. (1980) and Swanson (1980) have provided for most of the factors in their model. The local coordinating environment is modeled by p_o which accounts not only for the coordination number of bridging oxygen but also distinguishes among different types of coordinating atoms to some extent in terms of their formal valence and coordination number.

Thus, p_o implicitly accounts for the "linkage factor" noted in alkali feldspars (Clark and Papike 1967; Ribbe et al. 1974) due to the differences in classical electrostatic bond strengths contributed to oxygen by Al and Si. It also distinguishes between nontetrahedral atoms of different valence, e.g., Na and Ca. However, it cannot distinguish between atoms of the same valence and coordination number, e.g., Na and K. The dependence of r(SiO) on p_o was first noted in the melilite structure (Smith 1953). A strong linear dependence on p_o has since been quantified by Baur (1970; 1981) for r(SiO) and r(AlO) as well as a number of other bond types. One might think that a parameter such as $\Sigma[1/r(XO)^2]$ ($r(XO)$ = nontetrahedral bond length) as devised by Phillips et al. (1973) in a study of bond length variations in anorthite would be better than p_o for characterizing the effect of the nontetrahedral atoms. $\Sigma[1/r(XO)^2]$ was found to be a very sensitive parameter for r (SiO) and r(AlO) variation in that study. In a review of tetrahedral bond length variations in feldspars, Ribbe et al. (1974) also noted $\Sigma[1/r(XO)^2]$ to be an important parameter in monoclinic K-rich feldspars and sodic plagioclases as well as anorthite. However, in our analyses of either feldspars as a group or framework silicates in general, $\Sigma[1/r(XO)^2]$ is not a significant parameter in the presence of p_o.

In modeling the angular environment, Swanson (1980) chose f_s (O) which for the moment we will simply consider as a convenient linearizing function of the TOT angle. However, he did not parameterize OTO angle variations. We will demonstrate that the OTO angle variation is an important parameter for r(SiO) and r(AlO) variations.

In view of the success of the Swanson et al. (1980) and Swanson (1980) model and as an extension of these studies, we will continue to model r(SiO) and r(AlO) variations using the parameters p_o and f_s(O), and an additional parameter $f_s(T)$. $f_s(T)$ is the fractional s-character of the tetrahedral atom and is defined in the same fashion as f_s(O) such that $f_s(T) = 1/(1\text{-sec} < \angle OTO >)$ where $< \angle OTO >$ is the average of the three OTO angles formed with the bridging TO bond (Louisnathan and Gibbs 1972a; Louisnathan et al. 1977). What is required at this point is some consistent interpretation of the relationships these parameters have with the TO bond. Each of the parameters p_o, f_s(O), and $f_s(T)$ has a specific bonding model associated with it. For example, p_o is the sum of the strengths of electrostatic bonds as defined by Pauling's (1929) electrostatic valence rule. In contrast to p_o, fractional s-characters f_s(O) and $f_s(T)$ are measures of the hybridization state of the O and T atom, respectively. The negative secant of the angle defines the degree of mixing of s- and p-type atomic orbitals on the atom (Coulson 1961; Newton and Gibbs 1980; Newton 1981).

Rather than try to interpret p_o, f_s(O), and $f_s(T)$ in terms of their original definitions, we can examine these parameters using the results of MO calculations. MO methods provide electron population analyses which can be used to partition the total number of electrons in a system into atomic and bond contributions (Mulliken 1932; 1935; 1955). The bond contribution, referred to as the Mulliken overlap population $n(TO)$, provides some measure of the covalent strength of a bond (Mulliken 1955). Larger positive values of $n(TO)$ suggest stronger covalent interactions and shorter bonds whereas values of $n(TO)$ near zero suggest a more ionic interaction and longer bonds (Newton 1981). Since bond length can be correlated with bond strength (see Brown and Shannon 1973), we should observe a correlation between overlap population and bond length if overlap populations represent some measure of bond strength. This is exactly as has been observed in previous MO studies (e.g. Gibbs et al. 1972; Lager and Gibbs 1973; Gibbs et al. 1974; Hill et al. 1977; Newton and Gibbs 1980; Gibbs et al. 1981; Burdett and McLarnan, 1984). With increasing overlap population, a decrease in bond length is observed. Using the overlap population as a measure of covalent strength of or of the quantity of electron density serving to bind two nuclei together, one can interpret a larger overlap population in a given TO bond as an indication of a stronger TO bond which manifests itself in a shorter TO bond length.

Each of the factors we have chosen to model bond length variation in SiO and AlO bonds has been examined in one form or another in terms of Mulliken overlap populations in previous MO studies. For example, in a study of geometries in minerals using extended Huckel MO techniques, Tossell and Gibbs (1977) found that for an increase in the average of the three OTO angles common to the TO bond in nontransition metal tetrahedral oxyanions TO_4^{n-} (T = Li, Be, B, Al, P, S, Ga, Ge, As, Se), $n(TO)$ increases as $r(TO)$ decreases. Several studies demonstrated correlations between TOT angles and $n(TO)$ such that with increasing angle the overlap population increases and $r(TO)$ decreases (e.g., Gibbs et al. 1972; Gibbs et al. 1974; Tossell and Gibbs 1977; Newton and Gibbs 1980; Gibbs et al. 1981). Recently, Gibbs (1982) demonstrated a strong linear correlation between the Pauling bond strengths and Mulliken overlap populations such that with increasing overlap population, there is an increase in the Pauling bond strength. Thus, it is apparent (Gibbs et al. 1972; Gibbs 1982) that Pauling's rules can be interpreted equally well either in terms of a covalent parameter like bond overlap population or in terms of an ionic parameter like the electrostatic bond strength (Pauling 1960; Bent 1968). In connection with this, Brown and Shannon (1973) recognize that the concept of bond strength usually associated with an ionic model works just as well in situations dealing with primarily covalent bonding. Furthermore, they demonstrate their empirical bond strengths to be related to oxide bond covalency.

The correlation between Pauling bond strength and $n(TO)$ suggests that a correlation should exist between the sum of the Pauling bond strengths p_o and n(SiO) and n(AlO). Louisnathan and Gibbs (1972b) and Cameron and Gibbs (1973), for example, have published such correlations for p_o and n(SiO) calculated with semi-empirical methods. We confirm the correlation by plotting $n(TO)$ for SiO and AlO bonds as a function of p_o in Figure 7, using the calculated overlap populations and p_o's for the molecules listed in Tables 1–3. Negative correlations are well-developed for both the SiO ($r^2 = 0.91$) and AlO ($r^2 = 0.87$) bonds. Note that the AlO bonds have smaller overlap populations than the SiO bonds consonant with the belief that an AlO bond possesses less covalent character than a SiO bond.

In light of the relationships between (1) $n(TO)$ and $r(TO)$, and (2) $n(TO)$ and the parameters chosen to model $r(TO)$, we make the following observation. Mulliken overlap populations can provide a consistent method for interpreting the relationship between local environment and bond length variation. In other words, the type and number of atoms around the bridging oxygen (characterized by p_o) and the positioning of these atoms around the bond (char-

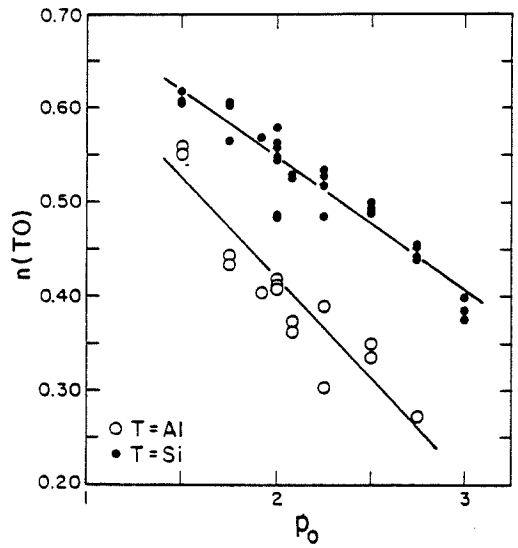

Fig. 7. MO calculated Mulliken overlap populations of the bridging *T*O bonds $n(TO)$ (T=Al, Si) vs. the sum of the Pauling bond strengths to the bridging oxygen. Aluminate data are plotted as open circles and silicate data as filled circles. These data were obtained from the non-empirical MO calculations on the molecules listed in Tables 1–3. Solid lines represent the regression lines for these data

acterized by the angular environment, $f_s(O)$ and $f_s(T)$) can be related through overlap populations to regular variations in the strength of the tetrahedral bond which manifest themselves as variations in the bond length.

In the remainder of this study, we will examine the relationships that obtain between p_o, $f_s(O)$ and $f_s(T)$, and $r(TO)$ using simple and multiple linear regression techniques on both theoretical and experimental bond length data. Regression techniques are ideally suited to this kind of study as they provide a systematic method for testing, with confidence limits, whether the bond length data are consistent with the hypothesis that they correlate with p_o, $f_s(O)$ and $f_s(T)$. In view of all the previous theoretical and empirical studies on different molecular and mineral systems, there is no doubt we will observe correlations. The point of this examination is to bring various ideas together in one comprehensive examination of SiO and AlO bond length variation in framework structures. The regression analyses will be used to compare the similarities and differences in the responses of SiO and AlO bonds to their local environments and to perhaps indicate where our parameters fail to accurately model bond length variation.

Regression Analyses on SiO and AlO Bond Lengths from Theoretical Data

The molecules listed in Tables 1–3 provide the theoretical data base upon which we will test the dependence of $r(SiO)$ and $r(AlO)$ variation on the parameters p_o, $f_s(O)$, and $f_s(T)$. The advantage of first examining theoretical data is that random and systematic measurement errors usually associated with experimental data are absent. Moreover, as our parameters model local environment, they must first provide a good model in a molecular system if they are expected to hold for a complex crystal system. However, the theoretical data are biased to some extent because we have used

Table 6. Results of regression analyses for $r(SiO)_{opt}$. (1)–(3) are linear regressions to test dependence on individual parameters p_o, $f_s(O)$ and $f_s(T)$. (4) is multiple linear regression to model $r(SiO)_{opt}$ and test significance of parameters in each others presence. Statistics provided inlcude: (a) parameter estimates (intercepts and slopes), (b) estimated standard deviations (esd), (c) student's t statistic for rejecting the null hypothesis (t for H_o), (d) significance level for rejecting H_o (prob > t), and (e) coefficient of determination (r^2)

Variable	Parameter estimate	esd	t for H_o: parameter estimate = 0	prob > |t|	r^2
(1) intercept	1.415	0.011	119.690	0.0001	0.89
p_o	0.098	0.005	19.467	0.0001	
(2) intercept	1.888	0.048	39.053	0.0001	0.37
$f_s(O)$	−0.670	0.132	−5.148	0.0001	
(3) intercept	2.005	0.113	17.683	0.0001	0.17
$f_s(T)$	−1.445	0.449	−3.216	0.0024	
(4) intercept	1.560	0.054	29.098	0.0001	0.92
p_o	0.087	0.006	15.378	0.0001	
$f_s(O)$	−0.196	0.056	−3.501	0.0011	
$f_s(T)$	−0.184	0.159	−1.159	0.2530	

a minimal basis set in the calculations and have often constrained local symmetry or geometry. At the very least, the non-empirical method provides a consistent measurement of the bond lengths and angles. The molecules provide 47 SiO bond lengths and 18 AlO bond lengths for linear regression analysis. This is a larger data set than that used by Swanson et al. (1980), Swanson (1980), and Meagher et al. (1980) (14 SiO data and 8 AlO data), so comparison of slopes should be more realistic.

In the analyses of the optimized SiO bond lengths $r(SiO)_{opt}$, and AlO bond lengths, $r(AlO)_{opt}$, linear regressions were performed with each of these bond lengths expressed as a linear function of p_o, $f_s(O)$, and $f_s(T)$ (analyses (1), (2) and (3), respectively) and, in multiple linear regressions, as a linear combination of all three parameters (analysis (4)). Results of these regression analyses for $r(SiO)_{opt}$ and $r(AlO)_{opt}$ are provided in Tables 6 and 7, respectively. As expected, there are positive correlations of $r(SiO)$ and $r(AlO)$ with p_o and negative correlations with both $f_s(O)$ and $f_s(T)$. In our interpretations of these parameters, the correlations indicate an increase in the strengths of the individual SiO and AlO bonds with smaller p_o and with wider angles.

The parameter p_o provides the best single description of the variation in bond length, describing over 85% of the variation (as indicated by the coefficient of determination r^2) in both $r(SiO)$ and $r(AlO)$ in terms of a linear model. Each of the parameters p_o, $f_s(O)$, and $f_s(T)$ is significant at a 98% confidence level when individually modeling variation in $r(SiO)$ and $r(AlO)$. The significance is indicated by the probability > |t| column in Tables 6 and 7.

When using all three parameters to model $r(SiO)$ and $r(AlO)$ in multiple linear regression analyses (analysis (4) in Tables 6 and 7), 92% of the variation in $r(SiO)$ and 99% of the variation in $r(AlO)$ can be described in terms of a linear model. Both p_o and $f_s(O)$ are significant in the presence of all three parameters (at >99% level). However, in the case of $r(SiO)$, the null hypothesis that the slope is equal to zero for $f_s(T)$ can be rejected at the ~75%

Table 7. Results of regression analyses for $r(AlO)_{opt}$. (1)–(3) are linear regressions to test dependence on individual parameters p_o, $f_s(O)$ and $f_s(T)$. (4) is multiple linear regression to model $r(AlO)_{opt}$ and test significance of parameters in each others presence. Statistics provided include: (a) parameter estimates (intercepts and slopes), (b) estimated standard deviations (eds), (c) student's t statistic for rejecting the null hypothesis (t for H_o), (d) significance level for rejecting H_o (prob $> t$), and (e) coefficient of determination (r^2)

Variable	Parameter estimate	esd	t for H_o: parameter estimate = 0	prob $> \|t\|$	r^2
(1) intercept	1.464	0.027	53.860	0.0001	0.86
p_o	0.130	0.013	9.790	0.0001	
(2) intercept	1.978	0.065	30.365	0.0001	0.49
$f_s(O)$	−0.639	0.163	−3.916	0.0012	
(3) intercept	1.981	0.103	19.316	0.0001	0.28
$f_s(T)$	−1.044	0.417	−2.504	0.0235	
(4) intercept	1.739	0.024	71.678	0.0001	0.99
p_o	0.101	0.005	20.623	0.0001	
$f_s(O)$	−0.247	0.032	−7.747	0.0001	
$f_s(T)$	−0.489	0.062	−7.873	0.0001	

confidence level. Also note when modeling both $r(SiO)$ and $r(AlO)$ with one parameter alone, $f_s(T)$ is the least significant of the three parameters. We believe that this is due to bias in our data set. Unfortunately, in optimizing the various molecules, the majority of the OTO angles were fixed at 109.47° due to the great time and expense associated with a complete optimization of all the molecules. If we calculate linear regression analyses of $r(SiO)_{opt}$ and $r(AlO)_{opt}$ as a function of $f_s(T)$ using only those molecules where the OTO angles were optimized (15 SiO data and 7 AlO data), we find much better correlations. For these limited data sets, $f_s(T)$ accounts for 60% of the variation in $r(SiO)_{opt}$ with $r(SiO)_{opt} = 1.95 - 1.3f_s(T)$. For $r(AlO)_{opt}$, $f_s(T)$ accounts for 87% of the variation in $r(AlO)_{opt}$ with $r(AlO)_{opt} = 2.0 - 1.2f_s(T)$. In both of these analyses, the null hypothesis that the slope is zero can be rejected only at the 99% level.

Comparison of the slopes of p_o, $f_s(O)$, and $f_s(T)$ in analyses (1) through (3) to the corresponding slopes in the multiple linear regression analyses shows that the slopes in the individual regression analyses have greater magnitudes than the corresponding slopes in the multiple linear regression analyses (analysis (4)). This is true for both the SiO and AlO analyses in Tables 6 and 7. Thus, bond length variation shows a greater dependence on a given parameter when that parameter is entered into the regression analysis alone than when it is entered in conjunction with the other parameters. Obviously, variations in the individual parameters are not independent measures of bond length variation. Furthermore, the excellent correlations observed between bond length and p_o, for example, do not occur simply because p_o is the most important factor determining bond length but must also be related to the fact that the parameters are not independent. This is indicated by the moderate non-zero correlation coefficients between the independent variables in the multiple linear regression analyses (Table 8). In other words, when p_o is used alone to model bond length variation, p_o must to some extent implicitly account for the other factors associated with bond length variation.

Table 8. Correlation of independent parameters in multiple linear regression analyses for: (a) $r(SiO)_{opt}$ and (b) $r(AlO)_{opt}$

		p_o	$f_s(O)$	$f_s(T)$
(a)	p_o	1.0000	0.4782	0.3726
	$f_s(O)$		1.0000	0.0224
	$f_s(T)$			1.0000
(b)	p_o	1.0000	0.4542	0.1735
	$f_s(O)$		1.0000	−0.1698
	$f_s(T)$			1.0000

For example, from the analysis of TOT angles in the first section of this study, we know that a TOT angle may decrease with an increase in coordination number of the bridging oxygen from two to three. This is particularly true for two-coordinate TOT groups with flat potential energy curves such as SiOSi, SiOAl, and AlOAl. Both an increase in bridging-oxygen coordination number (increase in p_o) and a decrease in TOT angle (decrease in $f_s(O)$) are associated with a longer TO bond length. However, that p_o alone cannot implicitly account for all the variations in the local environment of a TO bond is indicated by the better coefficients of determination obtained when using $f_s(O)$ and $f_s(T)$ in addition to p_o in modeling $r(TO)$ variation with a multiple linear regression analysis. Moreover, variations in p_o cannot account for variations in $r(SiO)$ in the olivines and the silica polymorphs where $r(SiO)$ is correlated inversely with $f_s(T)$ and $f_s(O)$ and where p_o is exactly 2.0 (Louisnathan and Gibbs 1972b; Gibbs et al. 1972).

In comparing the slopes of each of the parameters defining the $r(SiO)_{opt}$ and $r(AlO)_{opt}$ (regression (4), Tables 6 and 7), one can see that the slopes for corresponding parameters in both regressions are roughly similar. This may suggest that the SiO and AlO bond lengths vary in a similar fashion in the same local environment and might be treated as a single population if the Al-content is taken into account. We cannot realistically compare the slopes for $f_s(T)$ due to the bias in the data. However, from the simple linear regressions described in the previous paragraph where only optimized OTO angle data were employed, one can see that the slope for $f_s(T)$ is steeper for the SiO data than for the AlO data as observed earlier by Tossell and Gibbs (1977). This suggests that AlO bond lengths do vary in a different fashion than SiO bond lengths in a similar environment. The consequence of this difference will be discussed further when examining observed bond lengths from experimental data.

The dependence of $r(SiO)_{opt}$ and $r(AlO)_{opt}$ on each of the parameters p_o, $f_s(O)$, and $f_s(T)$ is displayed in Figures 8a, b, and c, respectively. Examination of the plotted points in Figure 8c indicates the large number of data which were fixed at $f_s(T) = 0.25$ (OTO angle = 109.47°). Figure 8d is a diagram of bond lengths calculated as a function of p_o, $f_s(O)$, and $f_s(T)$ ($r(TO)_{calc}$) using the separate multiple regression equations for $r(SiO)_{opt}$ and $r(AlO)_{opt}$ plotted against the actual optimized SiO and AlO bond lengths ($r(TO)_{opt}$). We stress that although the SiO and AlO data are plotted on the same diagram, the calculated bond lengths were determined using the separate multiple regression equations for the SiO and AlO data. In other words, we have in no way attempted to treat the optimized data as a single population by modeling for average Al content.

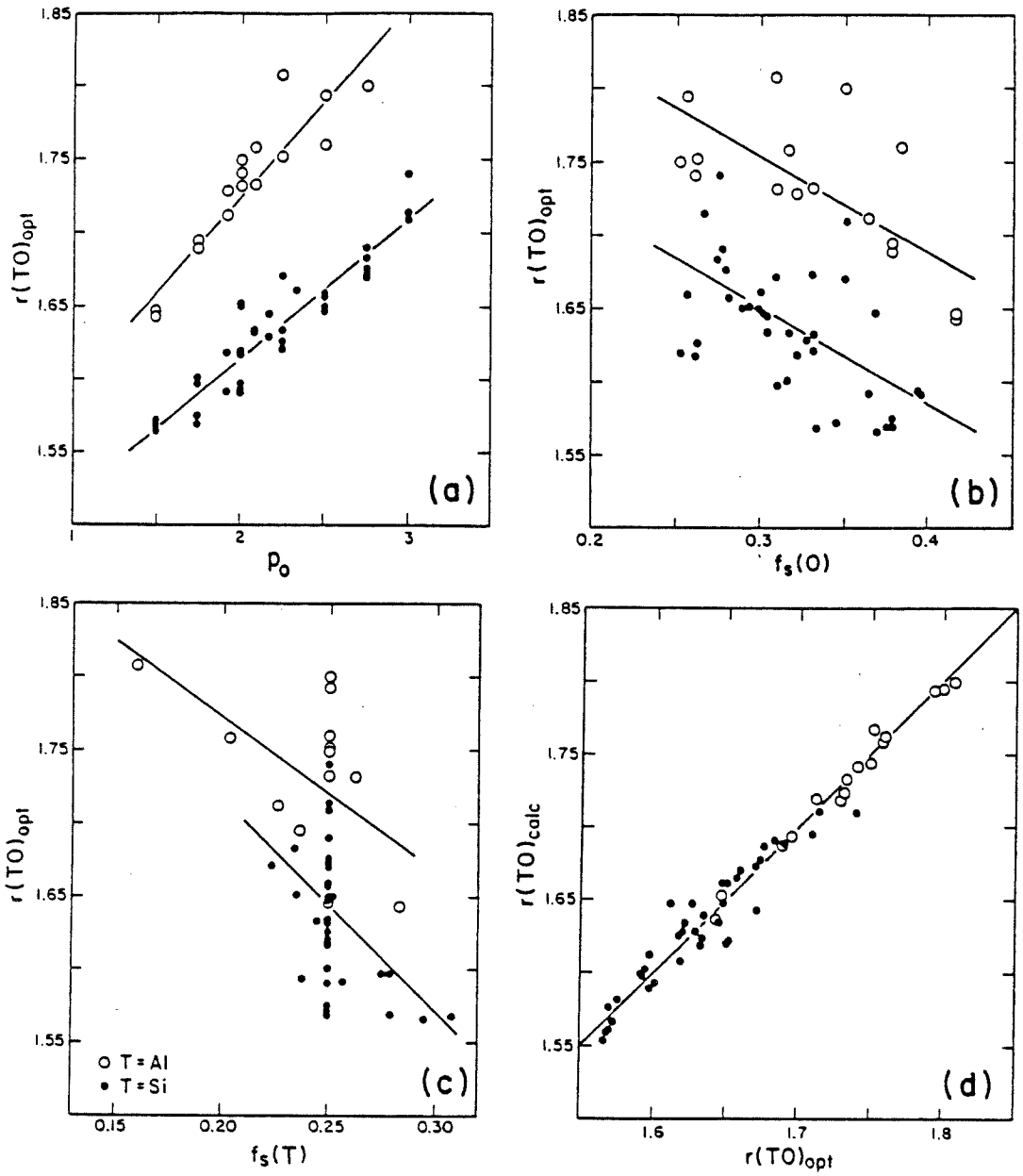

Fig. 8a–d. Optimized tetrahedral *TO* (T=Si, Al) bond lengths, $r(TO)_{opt}$, displayed as a function of: (**a**) the Pauling bond strength sum to the bridging oxygen atom, p_o, (**b**) the fractional s-character of the bridging oxygen atom, $f_s(O)$, and (**c**) the fractional s-character of the tetrahedral atom, $f_s(T)$. The aluminate data are represented by open circles and silicate data by filled circles. In (**a**), (**b**), and (**c**), solid lines represent the regression lines (equations listed in Tables 6 and 7, analyses (1)–(3)) calculated from these molecular data. In (**d**), tetrahedral bond lengths $r(TO)$ calc, calculated as a linear combination of p_o, $f_s(O)$, and $f_s(T)$ are plotted as a function of the optimized bond lengths, $r(TO)_{opt}$. Separate multiple linear regression equations (analyses (4), Tables 6 and 7) were used to calculate $r(SiO)_{opt}$ and $r(AlO)_{opt}$. The solid line represents a line of perfect agreement in (**d**)

Examination of Figure 8d indicates that using only the parameters p_o, $f_s(O)$, and $f_s(T)$ as a model for bond length variation in molecular systems serves to rank the bond lengths fairly well. The maximum deviation from the line of perfect agreement for the SiO data is 0.03 Å while that for the AlO data is somewhat less than 0.01 Å, well within the error expected for such calculations.

Regardless of how well we have modeled bond length variation using only p_o, $f_s(O)$, and $f_s(T)$, it is important to question where the model may be inadequate or how it might be improved. For example, is a linear model appropriate? In the case of angular parameters, we have attempted to linearize the dependence of bond length on angle by using functions of the angles, $f_s(O)$ and $f_s(T)$, as opposed to the angles themselves. That bond length should vary more or less linearly with fractional *s*-character, all other things being equal, has been argued by Dewar and Schmeising (1960) in a study of carbon compounds. Newton and Gibbs (1980) have rigorously demonstrated a linear relationship between $r(SiO)$ and $f_s(O)$ in $H_6Si_2O_7$ which is obeyed by the bond length variations in the silica polymorphs (Hill and Gibbs 1979). On the other hand, we have no prior knowledge that bond length must vary linearly with p_o except for the following three facts: (1) the linear

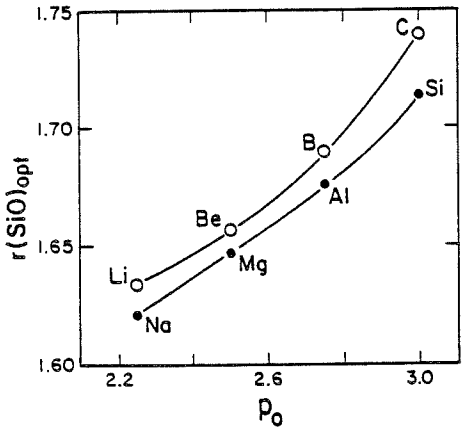

Fig. 9. Optimized tetrahedral SiO bond lengths, $r(SiO)_{opt}$, from $X(OH)_3$–$H_6Si_2O_7$ molecules are displayed as a function of Pauling bond strength sum to the bridging oxygen, p_o. First row and second row X atoms are plotted as open and filled circles, respectively. The solid lines have no functional significance but have simply been included to separate the molecules containing first row from second row X atoms

relationship between overlap population and p_o (Fig. 7); (2) the linear relationship between $n(TO)$ and $r(TO)$ observed by Tossell and Gibbs (1977); and (3) the linear relationships between p_o and bond length provided by Baur (1970, 1981). Indeed, the well-known bond strength-bond length relationships determined by Brown and Shannon (1973) indicate a curvilinear relationship between bond length and bond strength. Brown and Shannon (1973) suggest that Baur's (1970) linear regressions are reasonable approximations in the examples he studied because the average bond lengths for the structures studied are nearly constant from one site to another. For example, Si and Al in tetrahedral coordination only exhibit small distortions of their coordination polyhedra. Thus, a linear approximation is sufficient to model the variation. This is supported by the well-developed linear dependence of $r(SiO)_{opt}$ and $r(AlO)_{opt}$ on p_o in our molecular systems where Al and Si are both four coordinate.

However, it is still worthwhile examining the effects of p_o on bond length, everything else being equal. The MO calculations allow a separation of p_o effects whereas, in examination of experimental bond lengths, one does not have this advantage. For an analysis of this type, we can use some of the $X(OH)_3$–$H_6Si_2O_7$ molecules listed in Table 2. Note that each of these molecules has the same TOT (SiOSi) group. Also, if only those molecules with OTO angles fixed at 109.47° are used, then the intrinsic effects of the OTO variations are effectively eliminated. Also, the TOT angles for these molecules are all very nearly equal to 120° so the intrinsic effects of TOT variation are effectively eliminated as well. Each of the coordinating X atoms is four-coordinate and there is only one X atom coordinated to bridging oxygen in each molecule. Therefore, variation in coordination number is eliminated. The change in p_o in these molecules is only related to a change in the formal valence of the X atom. These molecules actually provide two series for examination X=Li, Be, B, C and X=Na, Mg, Al, Si.

Figure 9 demonstrates the dependence of bond length on p_o in these molecules. Although the errors on the optimized SiO bond lengths may be on the order of 0.03 Å (Pople 1982; Carsky and Urban 1980), the systematic variation of the bond lengths related to the position of the X atom in the periodic table suggests that $r(SiO)$ does not vary linearly with p_o. Bond length changes more rapidly from left to right in the periodic table. Moreover, atoms in the first row (Li, Be, B, C) lengthen the bond length more than atoms in the second row (Na, Mg, Al, Si). The limited available data also suggest that the same kinds of trends obtain for SiO and AlO in SiOAl groups. Also, recall from the discussion of TOT angle variation that the range in SiOSi angle as indicated by potential energy curves is more restricted for a second period atom than a third period atom of the same valence and for atoms farther to the right within the same period. From Figure 9, we suggest that the parameter p_o does not adequately account for the intrinsic "chemistry" or electronic structure of different types of atoms. Efforts to model for this effect by including parameters such as electronegativity or ionization potentials were unsuccessful or at least provided inconsistent results in regression analyses. For example, including an average ionization potential of the additional atoms coordinated to an SiO bond through the bridging oxygen provided a slightly better model of $r(SiO)_{opt}$ variation with the coefficient of determination increasing from $r^2=0.92$ to 0.94. However, the same parameter was *not* significant in the presence of p_o, $f_s(O)$ and $f_s(T)$ for $r(AlO)_{opt}$. Whether our inability to consistently improve the model is due to the types of "chemical effect" parameters chosen, the manner in which the parameters were included in the regression analyses, or some limitation in the data itself is not clear. Until we can determine some method which better quantifies the effects of particular atomic types on bond length variation, we suggest that a linear model including p_o, $f_s(O)$, and $f_s(T)$ is adequate. The reader is reminded that when using only these three parameters to model for the local environmental effects on bond length, the results of the multiple linear regression analyses were quite good having accounted for 92% of the variation in $r(SiO)_{opt}$ and 99% of the variation in $r(AlO)_{opt}$.

Regression Analyses on SiO and AlO Bond Lengths in Framework Silicates

Having demonstrated that the parameters p_o, $f_s(O)$, and $f_s(T)$ provide a quantum chemical modeling of $r(SiO)$ and $r(AlO)$ variation in molecules, it remains to test the extent to which these parameters can model bond length variations in framework structures. The structures chosen for analysis include low quartz (Wright and Lehmann 1981; Stewart and Spackman, personal communication), low cristobalite (Peacor 1973), coesite (Gibbs et al. 1977; Geisinger 1983), low albite (Wainwright and Starkey, personal communication; Harlow and Brown 1980); low microcline (Brown and Bailey 1964; Strob, personal communication), anorthite (Wainwright and Starkey 1971), slawsonite (Griffen et al. 1977), and paracelsian (Craig et al. 1973). These structures provide 144 SiO and 78 AlO data. In the case of the aluminosilicates, only those structures that can be presumed to have a completely ordered Si/Al distribution were used. This is required in the analysis to eliminate any dependence of the mean TO bond length variation on the average Al/Si content of the tetrahedra. In the case of low microcline and low albite, there has been some debate as to whether or not these feldspars are completely ordered, with sug-

gested values of up to 15 to 20% disorder (cf. Ferguson et al. 1958; Gait et al. 1970; Ferguson 1979). However, neutron diffraction results for low albite (Harlow and Brown 1980), which indicate the structure to be completely ordered within experimental error, cannot be discounted. Furthermore, the average SiO bond length in framework aluminosilicates accepted as fully ordered is slightly less than 1.62 Å. With regard to this, 15 to 20% disorder should increase the average SiO bond length in low microcline and low albite to as high as ~1.64 Å. The average SiO bond length in both structures is less than 1.62 Å. Therefore, we regard low microcline and low albite as fully ordered within the experimental error.

Another point which might be argued is that since we are using silica polymorph structures as well as aluminosilicate structures to provide the SiO data, then perhaps aluminate structures should be included for the AlO data. Anhydrous aluminate framework structures do exist. However we have no evidence as to how accurate the crystallographic data are. For example, in recent refinements of $CaAl_2O_4$ (Horkner and Muller-Buschbaum 1976), $SrAl_2O_4$ (Schulze and Muller-Buschbaum 1981) and $BaAl_2O_4$ (Horkner and Muller-Buschbaum 1979), no error estimates are provided. Furthermore, in $BaAl_2O_4$, there is positional disorder of the O3 oxygen in the subcell (Perrotta and Smith 1968) while for $SrAl_2O_4$ there is some question as to whether different symmetry low- and high-temperature forms exist. Rather than include data of unknown accuracy, we have only used AlO data from aluminosilicates, perhaps resulting in a biased data set.

Regression analyses for the observed data from the framework structures listed above were undertaken in the same manner as for the theoretical molecular data. Linear regressions were calculated for observed bond lengths $r(SiO)_{obs}$ and $r(AlO)_{obs}$ both as a linear function of p_o, $f_s(O)$, and $f_s(T)$ (analyses (1)-(3), respectively). Likewise, multiple linear regression analyses were calculated for $r(SiO)_{obs}$ and $r(AlO)_{obs}$ as a linear combination of all three parameters (analysis (4)). Results of the regression analyses are provided in Tables 9 ($r(SiO)_{obs}$) and 10 ($r(AlO)_{obs}$).

In agreement with the results for the molecular data and previous empirical analyses of bond length variation, we observe a positive correlation of bond length variation with p_o and negative correlations with $f_s(O)$ and $f_s(T)$. Each of these parameters shows a significant correlation with $r(SiO)_{obs}$ and $r(AlO)_{obs}$ variation. As in the previous section, the parameter p_o alone provides an important description of both $r(SiO)$ and $r(AlO)$ variation accounting in both cases for over 55% of the variation in terms of a linear model. Note also that the parameter $f_s(T)$ is significantly correlated with bond length variation. Indeed, in the case of $r(SiO)_{obs}$ variation, $f_s(T)$ provides the best single description of the bond length variation accounting for 60% of the variation in terms of a linear model.

Using all three parameters in multiple linear regression analyses (analysis (4) in Tables 9 and 10) accounts for 76% and 79% of the variation in $r(SiO)_{obs}$ and $r(AlO)_{obs}$, respectively. Moreover, each of the parameters is highly significant in the presence of the others. The null hypothesis that the slopes are equal to zero can be rejected at better than the 99% level. As was true in the analysis of the molecular data, the slopes of p_o and f_s (O) for the SiO and AlO data are statistically identical. Although only hinted at in the molecular analysis, the slopes of $f_s(T)$ for $r(SiO)_{obs}$ and $r(AlO)_{obs}$ in the multiple linear regression analyses are undeniably different, at least for the data we have employed. This is an important result. In as much as $f_s(T)$ contributes significantly in modeling both $r(SiO)_{obs}$ and $r(AlO)_{obs}$, this type of parameter should not be ignored in modeling bond length variation. Moreover, as the slopes for $f_s(T)$ are different, it is inappropriate to treat SiO and AlO bond lengths as a single population tied together by a parameter accounting for Al content. In other words, SiO bond lengths and AlO bond lengths can vary differently in similar local environments. This result corroborates the work of Tossell and Gibbs (1977) who found the dependence of tetrahedral bond length variation to be better developed as the electronegativity of the tetrahedral atom increases. These com-

Table 9. Results of regression analyses for $r(SiO)_{obs}$. (1)–(3) are linear regressions to test dependence on individual parameters p_o, $f_s(O)$ and $f_s(T)$. (4) is multiple linear regression to model $r(SiO)_{obs}$ and test significance of parameters in each others presence. Statistics provided include: (a) parameter estimates (intercepts and slopes), (b) estimated standard deviations (esd), (c) student's t statistic for rejecting the null hypothesis (t for H_o), (d) significance level for rejecting H_o (prob > t), and (e) coefficient of determination (r^2)

Variable	Parameter estimate	esd	t for H_o: parameter estimate = 0	prob > |t|	r^2
(1) intercept	1.407	0.015	92.063	0.0001	0.56
p_o	0.102	0.008	13.510	0.0001	
(2) intercept	1.712	0.014	124.405	0.0001	0.27
$f_s(O)$	−0.229	0.320	− 7.168	0.0001	
(3) intercept	1.892	0.019	98.267	0.0001	0.60
$f_s(T)$	−1.117	0.077	−14.500	0.0001	
(4) intercept	1.727	0.036	48.466	0.0001	0.76
p_o	0.050	0.008	6.108	0.0001	
$f_s(O)$	−0.137	0.019	− 7.204	0.0001	
$f_s(T)$	−0.620	0.086	− 7.191	0.0001	

Table 10. Results of regression analyses for $r(AlO)_{obs}$. (1)–(3) are linear regressions to test dependence on individual parameters p_o, $f_s(O)$ and $f_s(T)$. (4) is multiple linear regression to model $r(AlO)_{obs}$ and test significance of parameters in each others presence. Statistics provided include: (a) parameter estimates (intercepts and slopes), (b) estimated standard deviations (esd), (c) student's t statistic for rejecting the null hypothesis (t for H_o), (d) significance level for rejecting H_o (prob > t), and (e) coefficient of determination (r^2)

Variable	Parameter estimate	esd	t for H_o: parameter estimate = 0	prob > |t|	r^2
(1) intercept	1.562	0.017	92.688	0.0001	0.61
p_o	0.091	0.008	10.863	0.0001	
(2) intercept	1.874	0.019	98.014	0.0001	0.38
$f_s(O)$	−0.312	0.046	−6.783	0.0001	
(3) intercept	1.895	0.022	86.959	0.0001	0.37
$f_s(T)$	−0.604	0.087	−6.921	0.0001	
(4) intercept	1.796	0.032	56.245	0.0001	0.79
p_o	0.054	0.008	6.834	0.0001	
$f_s(O)$	−0.183	0.030	−6.104	0.0001	
$f_s(T)$	−0.332	0.059	−5.593	0.0001	

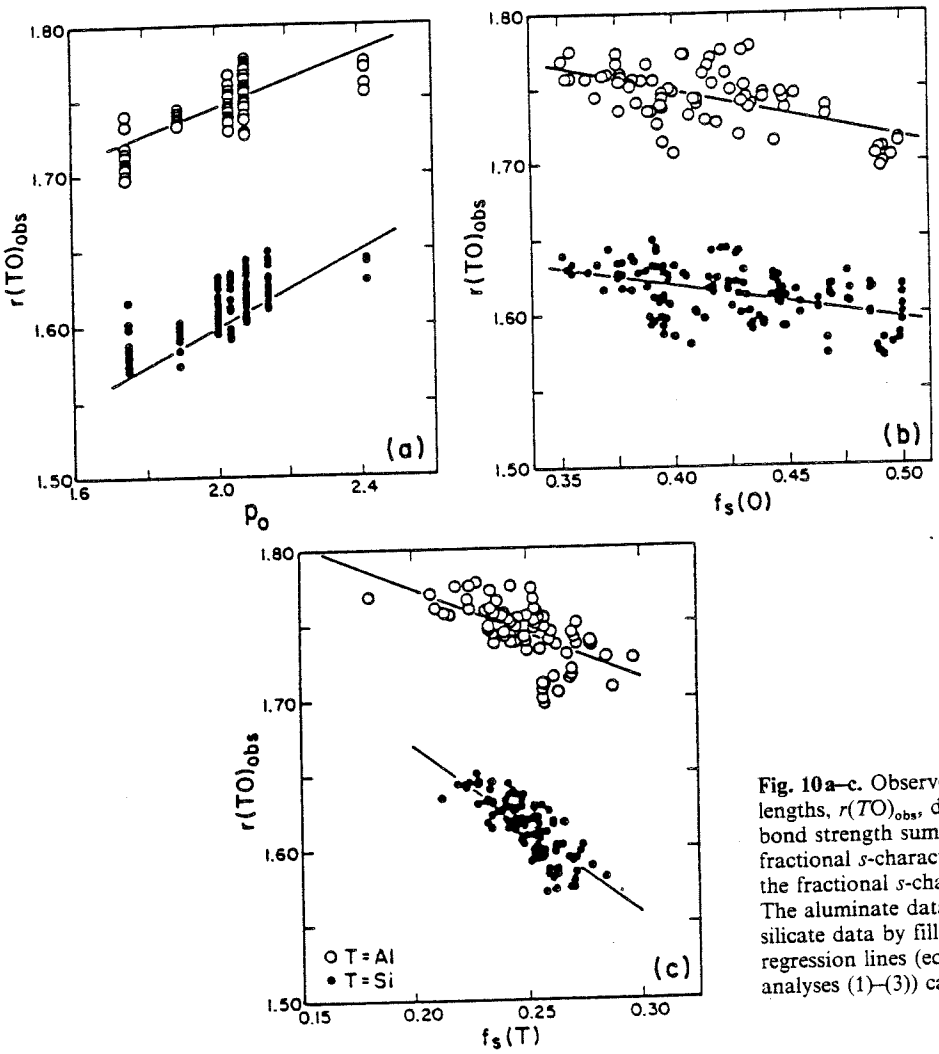

Fig. 10a–c. Observed tetrahedral *TO* (T=Si, Al) bond lengths, $r(TO)_{obs}$, displayed as a function of: (**a**) the Pauling bond strength sum to the bridging oxygen, p_o, (**b**) the fractional *s*-character of the bridging oxygen, $f_s(O)$, and (**c**) the fractional *s*-character of the tetrahedral atoms, $f_s(T)$. The aluminate data are represented by open circles and the silicate data by filled circles. Solid lines represent the regression lines (equations listed in Tables 9 and 10, analyses (1)–(3)) calculated from these experimental data

ments are directed primarily at preliminary empirical studies of r(Si, AlO) bond length variation undertaken by Swanson et al. (1980), Meagher et al. (1980), and Swanson (1980) and reported by Gibbs et al. (1981). In these studies, tetrahedral Al/Si bond length variation was modeled as a function of p_o, f_s(O) and x = the average Al content of the bond or tetrahedron. The fact that large coefficients of determination ($r^2 \simeq 0.99$) are obtained in this type of study is more a function of using two distinct populations of bond lengths – one short (r(SiO)) and one relatively longer (r(AlO)) – than resulting from accurate modeling of the local environment.

The dependence of observed SiO and AlO bond lengths on the parameters p_o, f_s(O), and $f_s(T)$ are displayed in Figures 10a, b, and c, respectively. One can easily observe the positive correlation with p_o and the negative correlations with f_s(O) and $f_s(T)$. The difference in slope for the SiO data compared to the AlO data as a function of $f_s(T)$ is also easily observable. In Figure 11a, bond lengths calculated from the multiple linear regression equations from the experimental data, $r(SiO)_{calc}$ and $r(AlO)_{calc}$, are plotted as a function of the observed bond lengths. As with the molecular data, we can see that a linear model for bond length variation incorporating p_o, f_s(O), and $f_s(T)$ ranks the observed bond lengths fairly well. The maximum deviation from the line of perfect agreement in Figure 11a is ~0.025 Å for both the SiO data and the AlO data. Moreover, even when calculating r(SiO) and r(AlO) using the multiple linear regression equations obtained for the theoretical data, we can order the experimentally observed bond lengths reasonably well although the theoretical calculations systematically underestimate observed AlO bond lengths in solids. This is demonstrated in Figure 11b where the maximum deviation from a line of perfect agreement is 0.025 Å for the SiO data and 0.038 Å for the AlO data.

In summarizing the results of this examination of observed r(SiO) and r(AlO) variation, we can make a few observations. Our ability to model over 75% of $r(SiO)_{obs}$ and $r(AlO)_{obs}$ variation using the same type of linear model employed fairly successfully in molecular systems corroborates the viewpoint that local forces determining these bond lengths are similar in molecules and solids. However, there are quantitative differences between the models for the molecular and solid data such as some differences in slope for the same parameter and better accounting of molecular bond length variation than bond length variation in solids. These differences are probably related to variety of factors some of which may be included in the following. First.

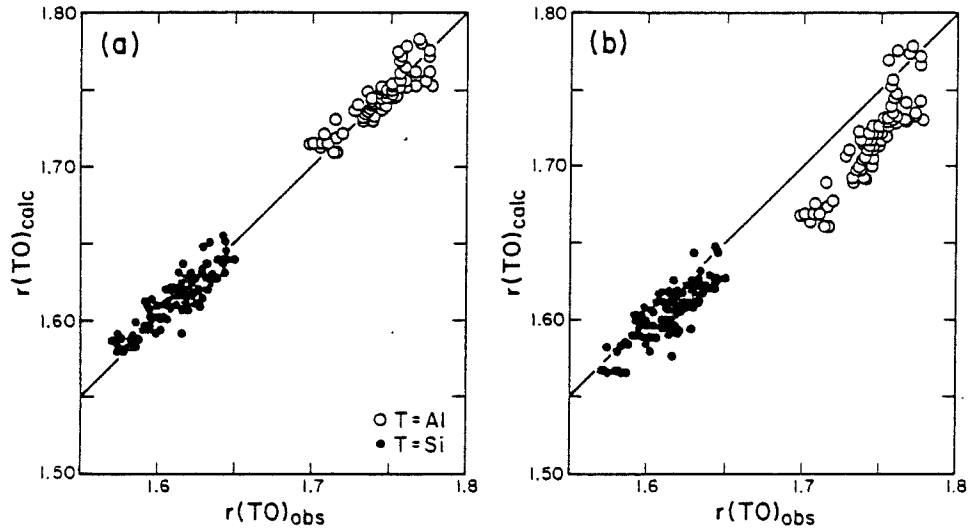

Fig. 11a, b. Tetrahedral *TO* (T=Si, Al) bond lengths, $r(TO)_{calc}$, calculated as a linear combination of the Pauling bond strength sum to the bridging oxygen atom, p_o, the fractional *s*-character of the bridging oxygen atom, $f_s(O)$, and the fractional *s*-character of the tetrahedral atom, $f_s(T)$. (**a**) Tetrahedral bond lengths, $r(TO)$ calc, calculated using separate multiple linear regression equations (listed in Tables 9 and 10, analyses (4)) from the observed silicate and aluminate data vs. the observed bridging bond lengths, $r(TO)_{obs}$, in framework structures. (**b**) Tetrahedral bond lengths, $r(TO)_{calc}$, calculated using separate multiple linear regression equations (listed in Tables 6 and 7, analyses (4)) from the theoretical molecular silicate and aluminate data vs. the observed bridging bond lengths, $r(TO)_{obs}$, in framework structures. The solid lines in (**a**) and (**b**) represent lines of perfect agreement

we have only attempted to explicitly model for bond length variation as a function of local environment. Certainly, the overall linkage of a structure affects the observed bond lengths (Smith and Bailey 1963). In addition, systematic errors that may be incurred by employing the minimal STO-3G basis set in the MO calculations will also contribute to differences between the models. Finally, with the random and systematic errors known to exist in experimental data, it is unlikely that we could obtain as good a correlation for the experimental data as we observed for the theoretical data, particularly when it is realized that the variation of r(SiO), for example, is less than an order of magnitude larger than its estimated error.

Although we indicated in the previous section that the parameter p_o may be inadequate in modeling the chemistry of the coordinating environment of the bridging oxygen, we do not believe that this is contributing very much to the smaller coefficients of determination in the observed data analyses. Using only silica polymorphs and aluminosilicates for the observed data, there is very little compositional variation in the frameworks. The majority of the variation comes from the nontetrahedral atoms modifying the aluminosilicate frameworks. These modifying atoms are generally in six-fold or higher coordination and are either alkali or earth-alkali elements. Thus, their effects on SiO or AlO bond lengths should not be as pronounced as the chemical effects demonstrated in the analysis of the theoretical data. Recall in that analysis, the atoms coordinated to the bridging oxygen of an SiOSi group were four-coordinate and included atoms ranging from Li to C and Na to Si. This serves to overemphasize the effects of changes in p_o on SiO bond lengths. In view of the good correlations obtained using p_o in the molecular system where the effects of p_o are emphasized, it is suggested that p_o will be a good model of the coordinating environment in the aluminosilicates which we have investigated.

Conclusions

Non-empirical MO calculations on molecules containing *TOT* (T=Si, Al, B, Be, Mg) groups have been used in this study to model and analyze variations in *TOT* angles and *TO* (T=Si, Al) bond lengths in solids. Examination of potential energy curves for two-coordinate oxygen *TOT* groups provides qualitative insight into the restrictions on the topology of a structure given a certain composition and the distribution of tetrahedral atoms into particular sites in a structure in terms of the compliancy of the *TOT* angle. Increased coordination of the bridging oxygen in a particular *TOT* group apparently serves to limit the range of energetically feasible angles. The degree to which angular variation is restricted in a given *TOT* group may be determined by the type of additional coordinating atom. For example, in the three-coordinate SiOSi groups examined, the energetic barrier to bending induced by the additional coordinating atom *X* is larger the more electronegative the *X* atom. This is not meant to imply that greater electronegativity of *X* causes the greater barrier. It is only used as one possible parameter to identify the trend.

In an analysis of SiO and AlO bond length variation, the parameters p_o, $f_s(O)$, and $f_s(T)$ have been demonstrated to provide good representations of bond length variation in molecules within the confines of linear models. These parameters have been used to model the local environment of the SiO and AlO bonds. Variations in bond length can be related through these parameters to variations in bond strength. We hasten to point out that we are not using the regression analyses to imply a direct cause and effect relationship between variations in each of these parameters and bond length variation. However, by using Mulliken overlap populations, one can associate overall changes in bond strength (and therefore bond length) with variations in these parameters. Close inspection of the parameter p_o

suggests that variation of bond length may not necessarily exhibit a linear dependence on p_o. For example, given an atom of the same valence and coordination number coordinated to the bridging oxygen of an SiOSi group, the group with the atom of greater electronegativity has longer bonds. Moreover, as one moves from left to right within one period of the periodic table, the dependence of SiO bond length on p_o is curvilinear in conformity with the Brown-Shannon bond strength-bond length curves.

Our ability to model SiO and AlO bond lengths in solids using the same parameters successfully tested in molecular systems has been demonstrated, using data from several silica polymorphs and framework aluminosilicates. The results indicate that in modeling bond length variations, all three parameters, p_o, $f_s(O)$ and $f_s(T)$, are important. The different slopes for $f_s(T)$ between the SiO and AlO multiple linear regression analyses suggest that SiO and AlO bond lengths should not be treated as a single population. Within the small compositional range of framework structures examined, we do not consider the possible nonlinear dependence of bond length on p_o to be a problem. However, if we hope to extend this type of model to structures with a larger variety of compositions, we must determine some method of better quantifying the "composition" of the local environment. This is particularly true for structures containing second period atoms.

Acknowledgements. We are indebted to the National Science Foundation for supporting this study with Grant EAR-8218743 and Virginia Tech and Arizona State University for contributing generous sums of monies to help defray the large computing costs incurred in our calculations. Part of this study was completed while one of us (GVG) was a Visiting Distinguished Professor of Chemistry at ASU during 1983. It is a pleasure to thank Bryan Chakoumakos, Paul McMillan, and an anonymous reviewer for reading and offering constructive criticisms of the manuscript. We thank Jody Bolen for typing the tables and correcting the final script file and Sharon Chiang for drafting figures.

References

Almenningen A, Bastiansen O, Ewing V, Hedberg K, Traetteberg M (1963) The molecular structure of disiloxane, $(SiH_3)_2O$. Acta Chem Scand 17:2455–2460

Appleman DE, Clark JR (1965) Crystal structure of reedmergnerite, a boron albite, and its relation to feldspar crystal chemistry. Am Mineral 50:1827–1850

Barrow MJ, Ebsworth EAV, Harding MM (1979) The crystal and molecular structures of disiloxane (at 108K) and hexamethyldisiloxane (at 148K). Acta Crystallogr Sect B 35:2093–2099

Baur WH (1970) Bond length variation and distorted coordination polyhedra in inorganic crystals. Trans Am Crystallogr Assoc 6:125–155

Baur WH (1981) Interatomic distance predictions for computer simulation of crystal structures. In: O'Keeffe M, Navrotsky A (eds) Structure and bonding in crystals II. Academic Press, New York, pp 31–52

Bent HA (1968) Ion-packing of covalent compounds. J Chem Ed 45:768–778

Binkley JS, Whiteside RA, Krishnan R, Seeger R, De Frees DJ, Schlegel HB, Topiol S, Kahn LR, Pople JA (1980) Gaussian 80 – An *ab initio* molecular orbital program. Department of Chemistry, Carnegie-Mellon University, Pittsburg, Pennsylvania 15213

Brown BE, Bailey SW (1964) The structure of maximum microcline. Acta Crystallogr 17:1391–1400

Brown GE, Gibbs GV, Ribbe PH (1969) The nature and variation in length of the Si–O and Al–O bonds in framework silicates. Am Mineral 54:1044–1061

Brown GE, Gibbs GV (1970) Stereochemistry and ordering the tetrahedral portion of silicates. Am Mineral 55:1587–1607

Brown ID, Shannon RD (1973) Empirical bond-strength – bond-length curves for oxides. Acta Crystallogr Sect A 29:266–281

Burdett JK, McLarnan TJ (1984) An orbital interpretation of Pauling's rules. Am Mineral 69:601–621

Cameron M, Gibbs GV (1973) The crystal structure and bonding in fluortremolite: A comparison with hydroxyl tremolite. Am Mineral 58:879–888

Carsky P, Urban M (1980) *Ab initio* calculations. Methods and applications in chemistry. Lecture notes in chemistry 16. Springer, Berlin Heidelberg New York

Chang KJ, Froyen S, Cohen ML (1983) The electronic band structures for zincblende and wurtzite BeO. J Phys Sect C: Solid State Phys 16:3475–3480

Clark JR, Papike JJ (1967) Silicon-oxygen bonds in chain and framework silicates (abstr). Progr Am Crystallogr Assoc Summer Meet Minneapolis 1967:91

Cohen JP, Ross FK, Gibbs GV (1977) An x-ray and neutron diffraction study of hydrous low cordierite. Am Mineral 62:67–78

Cole WF, Sorum H, Kennard O (1949) The crystal structure of orthoclase and sanidinized orthoclase. Acta Crystallogr 2:280–287

Coulson CA (1961) Valence. Oxford University Press, London

Craig JR, Louisnathan SJ, Gibbs GV (1973) Al/Si order in paracelsian (abstr). Trans Am Geophys Union 54:496

Cruickshank DWJ (1961) The role of 3d-orbitals ain π-bonds between (a) silicon, phosphorus, sulfur, or chlorine and (b) oxygen or nitrogen. J Chem Soc 1961:5486–5504

Dewar MJS, Schmeising HN (1960) Resonance and conjugation. – II. Factors determining bond lengths and heats of formation. Tetrahedron 11:96–120

Downs JW, Gibbs GV (1981) The role of the BeOSi bond in the structures of beryllosilicate minerals. Am Mineral 66:819–826

Eugster HP, McIver NL (1959) Boron analogues of alkali feldspars and related silicates (abstr). Geol Soc Am Bull 70:1598–1599

Ferguson RB (1979) Whence orthoclase and microcline? A crystallographer's interpretation of potassium feldspar phase relations. Can Mineral 17:515–525

Ferguson RB, Traill RJ, Taylor WH (1958) The crystal structures of low-temperature and high-temperature albites. Acta Crystallogr 11:331–348

Gait RI, Ferguson RB, Coish HR (1970) Electrostatic charge distribution in the structure of low albite, $NaAlSi_3O_8$. Acta Crystallogr Sect B 26:68–77

Geisinger KL (1983) A theoretical and experimental study of bonding in silicates and related materials. PhD dissertation, Virginia Polytechnic Institute and State University, Blacksburg, Virginia

Gibbs GV (1966) The polymorphism of cordierite. I. The crystal structure of low cordierite. Am Mineral 51:1068–1087

Gibbs GV (1982) Molecules as models for bonding in silicates. Am Mineral 67:421–450

Gibbs GV, Breck DW, Meagher EP (1968) Structural refinement of hydrous and anhydrous beryl, $Al_2(Be_3Si_6)O_{18}$, and emerald, $Al_{1.9}Cr_{0.1}(Be_3Si_9)O_{18}$. Lithos 1:275–285

Gibbs GV, Hamil MM, Louisnathan SJ, Bartell LS, Yow H (1972) Correlations between Si–O bond length, SiOSi angle and bond overlap populations calculated using extended Huckel molecular orbital theory. Am Mineral 57:1578–1613

Gibbs GV, Louisnathan SJ, Ribbe PH, Phillips MW (1974) Semiempirical molecular orbital calculations for the atoms of the tetrahedral framework in anorthite, low albite, maximum microcline and reedmergnerite. In: Mackenzie WS, Zussman J (eds) The feldspars. Manchester University Press, Manchester, pp 49–67

Gibbs GV, Prewitt CT, Baldwin KJ (1977) A study of the structural chemistry of coesite. Z Kristallogr 145:108–123

Gibbs GV, Meagher EP, Newton MD, Swanson DK (1981) A comparison of experimental and theoretical bond length and

angle variations for minerals, inorganic solids and molecules. In: O'Keefe M, Navrotsky A (eds) Structure and bonding in crystals I. Academic Press, New York, pp 195–225
Griffen DT, Ribbe PH, Gibbs GV (1977) The structure of slawsonite, a strontium analogue of paracelsian. Am Mineral 62:31–35
Gupta A, Tossell JA (1983) Quantum chemical studies of distortions and polymerization of borate polyhedra. Am Mineral 68:989–995
Harlow GE, Brown GE (1980) Low albite: An x-ray and neutron diffraction study. Am Mineral 65:986–995
Hehre WJ, Stewart RF, Pople JA (1969) Self-consistent molecular orbital methods. I. Use of Gaussian expansions of Slater-type atomic orbitals. J Chem Phys 51:2657–2664
Hehre WJ, Ditchfield R, Stewart RF, Pople JA (1970) Self-consistent molecular-orbital methods. IV. Use of Gaussian expansions of Slatertyp orbitals. Extension to second row molecules. J Chem Phys 52:2769–2773
Hill RJ, Gibbs GV (1979) Variation in d(T-O), d(T..T) and <TOT in silica and silicate minerals, phosphates and aluminates. Acta Crystallogr Sect B 35:25–30
Hill RJ, Louisnathan SJ, Gibbs GV (1977) Tetrahedral bond length and angle variations in germanates. Aust J Chem 30:1673–1684
Horkner W, Muller-Buschbaum HK (1976) Zur Kristallstruktur von $CaAl_2O_4$. J Inorg Nucl Chem 38:983–984
Horkner W, Muller-Buschbaum HK (1979) Zur Kristallstruktur von $BaAl_2O_4$. Z Anorg Allg Chem 451:40–44
Jones JB (1968) Al–O and Si–O tetrahedral distances in aluminosilicate framework structures. Acta Crystallogr Sect B: 24:355–358
Jones JB, Taylor WH (1968) Bond lengths in alkali feldspars. Acta Crystallogr Sect B: 24:1387–1392
Lager GA, Gibbs GV (1973) Effect of variations in O–P–O and P–O–P angles on P–O bond overlap populations for some selected ortho- and pyrophosphates. Am Mineral 58:756–764
Louisnathan SJ, Gibbs GV (1972a) The effect of tetrahedral angles on Si–O bond overlap populations for isolated tetrahedra. Am Mineral 57:1614–1642
Louisnathan SJ, Gibbs GV (1972b) Variation of Si–O distances in olivines, sodamelilite and sodium metasilicate as predicted by semi-empirical molecular orbital calculations. Am Mineral 57:1643–1663
Louisnathan SJ, Hill RJ, Gibbs GV (1977) Tetrahedral bond length variations in sulfates. Phys Chem Minerals 1:53–69
Meagher EP, Gibbs GV (1977) The polymorphism of cordierite. II. The crystal structure of indialite. Canad Mineral 15:43–49
Meagher EP, Swanson DK, Gibbs GV (1980) The calculation of tetrahedral SiO–O and Al–O bridging bond lengths and angles (abstr). Trans Am Geophy Union 61:408
Megaw HD, Kempster CJE, Radoslovich EW (1962) The structure of anorthite, $CaAl_2Si_2O_8$. II. Description and discussion. Acta Crystallogr 15:1017–1035
Mulliken RS (1932) Electronic structures of polyatomic molecules and valence. II. General considerations. Phys Rev 41:49–71
Mulliken RS (1935) Electronic structures of molecules. XI. Electroaffinity, molecular orbitals and dipole moments. J Chem Phys 3:573–585
Mulliken RS (1955) Electronic population on LCAO–MO molecular wave functions. II. Overlap populations, bond orders and covalent bond energies. J Chem Phys 23:1841–1846
Navrotsky A, Geisinger K, McMillan P, Gibbs GV (1985) The tetrahedral framework in glasses and melts – inferences from molecular orbital calculations and implications for structure, thermodynamics, and physical properties. Phys Chem Minerals 11:284–298
Newton MD (1981) Theoretical probes of bonding in the siloxy group. In: O'Keeffe M, Navrotsky A (eds) Structure and bonding in crystals I. Academic Press, New York, pp 175–193
Newton MD, Gibbs GV (1980) *Ab initio* calculated geometries and charge distributions for H_4SiO_4 and $H_6Si_2O_7$ compared with experimental values for silicates and siloxanes. Phys Chem Minerals 6:221–246
Pauling L (1929) The principles determining the structure of complex ionic crystals. J Am Chem Soc 51:1010–1026
Pauling L (1960) The nature of the chemical bond, 3rd edn. Cornell University Press, New York, pp 547–548 (Footnote 64)
Peacor DR (1973) High-temperature single-crystal study of the cristobalite inversion. Z Kristallorgr 138:274–298
Perrotta AJ, Smith JV (1968) The crystal structure of $BaAl_2O_4$. Bull Soc Fr Mineral Crystallogr 91:85–87
Phillips MW, Ribbe PH, Gibbs GV (1973) Tetrahedral bond length variations in anorthite. Am Mineral 58:495–499
Phillips MW, Gibbs GV, Ribbe PH (1974) The crystal structure of danburite: A comparison with anorthite, albite, and reedmergnerite. Am Mineral 59:79–85
Pople JA (1982) Molecular orbital theories and the structural properties of molecules. Ber Bunsenges Phys Chem 86:806–811
Pople JA, Gordon M (1967) Molecular orbital theory of the electronic structure of organic compounds. I. Subtituent effects and dipole moments. J Am Chem Soc 89:4253–4261
Pople JA, Hehre WJ, Lathan WA, Ditchfield R, Newton MD (1973) Gaussian 70: *Ab initio* ScF-MO calculations on organic molecules. Quantum chemistry program exchange 11:236. University of Indiana, Bloomington, Indiana
Ribbe PH, Gibbs GV (1969) Statistical analysis and discussion of mean Al/Si–O bond distances and the aluminium content of tetrahedra in feldspars. Am Mineral 54:85–94
Ribbe PH, Phillips MW, Gibbs GW (1974) Tetrahedral bond length variations in feldspars. In: Mackenzie WS, Zussman J (eds) The Feldspars. Manchester University Press, Manchester, pp 25–48
Roothaan CCJ (1951) New developments in molecular orbital theory. Rev Mod Phys 23:69–89
Schlegel HB (1982) Optimization of equilibrium geometries and transition structures. J Comput Chem 3:214–218
Schulze AR, Muller-Buschbaum HK (1981) Zur Struktur von monoklinem $SrAl_2O_4$. Z Anorg Allg Chem 475:205–210
Smith JV (1953) Reexamination of the crystal structure of melilite. Am Mineral 38:643–661
Smith JV (1954) A review of the Al–O and Si–O distance. Acta Crystallogr 7:479–481
Smith JV (1974) Feldspar minerals, Vol. 1. Springer, New York
Smith JV, Bailey SW (1963) Second review of Al–O and Si–O tetrahedral distances. Acta Crystallogr 16:801–811
Swanson DK, Meagher EP, Gibbs GV (1980) Calculation of tetrahedral and octahedral bond lengths for third row elements (abstr). Trans Am Geophys Union 61:409
Swanson DK (1980) A comparative study of *ab initio* generated geometries for first and second row atom oxide molecules with ocrresponding geometries in solids. MS thesis, Virginia Polytechnic Institute and State University, Blacksburg, Virginia
Tossell JA (1984) A qualitative MO model for bridging bond angle variations in minerals. Phys Chem Minerals 11:81–84
Tossell JA, Gibbs GV (1977) Molecular orbital studies of geometries and spectra of minerals and inorganic compounds. Phys Chem Minerals 2:21–57
Tossell JA, Gibbs GV (1978) The use of molecular-orbital calculations on model systems for the prediction of bridging-bond-angle variations in siloxanes, silicates, silicon nitrides and silicon sulfides. Acta Crystallogr Sect A 34:463–472
Wainwright JE, Starkey J (1971) A refinement of the structure of anorthite. Z Kristallogr 133:75–84
Wirght AF, Lehmann MS (1981) The structure of quartz at 25 and 590° C determined by neutron diffraction. J Solid State Chem 36:371–380

Received April 6, 1984